

# Dawn of Advanced Molecular Medicine: Nanotechnological Advancements in Cancer Imaging and Therapy

Charalambos Kaittanis, Travis M. Shaffer, Daniel L. J. Thorek & Jan Grimm\*

Molecular Pharmacology and Chemistry Program, Memorial Sloan-Kettering Cancer Center, New York, NY

\*Address all correspondence to: Jan Grimm, Molecular Pharmacology and Chemistry Program, Memorial Sloan Kettering Cancer Center, 1275 York Avenue, New York, NY 10065; Tel.: 646-888-3095; grimmj@mskcc.org

**ABSTRACT:** Nanotechnology plays an increasingly important role not only in our everyday life (with all its benefits and dangers) but also in medicine. Nanoparticles are to date the most intriguing option to deliver high concentrations of agents specifically and directly to cancer cells; therefore, a wide variety of these nanomaterials has been developed and explored. These span the range from simple nanoagents to sophisticated smart devices for drug delivery or imaging. Nanomaterials usually provide a large surface area, allowing for decoration with a large amount of moieties on the surface for either additional functionalities or targeting. Besides using particles solely for imaging purposes, they can also carry as a payload a therapeutic agent. If both are combined within the same particle, a theranostic agent is created. The sophistication of highly developed nanotechnology targeting approaches provides a promising means for many clinical implementations and can provide improved applications for otherwise suboptimal formulations. In this review we will explore nanotechnology both for imaging and therapy to provide a general overview of the field and its impact on cancer imaging and therapy.

**KEY WORDS:** nanoparticles, oncology, drug delivery, chemotherapy, targeted therapeutics

**ABBREVIATIONS:** **AuNP:** gold nanoparticle; **CNT:** carbon nanotube; **CT:** computed tomography; **EDC:** 1-ethyl-3-(3-dimethylaminopropyl)carbodiimide; **EPR:** enhanced permeability and retention; **FDG:** fluorodeoxyglucose; **IONP:** iron oxide nanoparticles; **MR:** magnetic resonance; **MRI:** magnetic resonance imaging; **NIR:** near-infrared; **nm:** nanometer; **NP:** nanoparticle; **PAT:** photoacoustic tomography; **PEG:** polyethylene glycol; **PET:** positron emission tomography; **PLGA:** poly(lactic-co-glycolic acid); **QD:** quantum dot; **RF:** radiofrequency; **SERS:** surface-enhanced Raman spectroscopy; **SPECT:** single-photon emission computed tomography; **SWCNTs:** single-walled carbon nanotubes; **T:** Tesla; **T1:** spin-lattice relaxation; **T2:** spin-spin relaxation; **UV:** Ultraviolet; **%ID/g:** percent injected dose per gram of tissue

## I. NANOTECHNOLOGY IN CANCER IMAGING

Nanotechnology is working with materials smaller than 100 nm. This includes a whole variety of organic as well as inorganic materials, including particles, dendrimers, wires, and tubes but also proteins and viruses to name just a few. Today, we can choose from this cornucopia of various agents to create nanomaterials suitable for both cancer diagnostics via imaging and even more for therapy or in combination of both in theranostic applications.<sup>1</sup> For these applications, several properties of the nanoparticles have to be carefully considered. Their size, surface charge, and shape as well as the biocompatibility of their components are of particular importance.

Nanomaterials usually provide a large surface-to-volume ratio, allowing for coupling a large amount of targeting (or therapeutic) moieties onto the material. Even weak, small organic molecules as ligands can significantly enhance the avidity of the particle toward its target by up to four orders of magnitude through multivalent interactions.<sup>2</sup> The size and the coating of materials determine their distribution in the body in addition to their solubility in aqueous media; polydispersed materials tend to have a much wider range of different elimination times than materials with a narrower size distribution. Besides using particles solely for imaging purposes, they can in addition also carry another payload: a therapeutic agent. In conjunction with the imaging moiety, this creates a theranostic agent. All this makes nanoma-

terials attractive platforms to utilize for a wide range of application in imaging and therapy of cancer.

### A. Nanoparticles for Optical Imaging

Optical approaches for molecular imaging and therapeutics utilize wavelengths that span from the ultraviolet (UV) through the visible spectrums and into the near-infrared (NIR) spectrum. Much of the nanoparticle work utilizing optical techniques such as luminescence, Raman, and fluorescence imaging have been focused on preclinical applications. This is because optical imaging, unlike clinical modalities such as X-ray or MR imaging, is depth dependent; optical wavelength light scatters and is absorbed by the biological medium through which it passes. Countering this disadvantage is the ease of use, high surface resolution, and diversity of probes in the optical domain. Nanoparticle (NP) approaches

further these advantages, providing greater stability, targeting, multiplexing capabilities, and ability to deliver cargo (Fig. 1). This section will discuss a variety of optical imaging techniques and discuss the different architectures, and chemical and materials properties (Fig. 2) of the NP for imaging and therapeutic applications.

### B. Fluorescence Imaging

The wavelength selective excitation of dyes and subsequent spectral discrimination of fluorescent emissions are among the most widely used tools in the biomedical sciences.<sup>3</sup> Most modern research institutions are equipped with at least some form of fluorescent microscope. Many now utilize these techniques for *in vivo* research as well. Fluorescent nanoparticle platforms have played a significant role in the expanding use of fluorescence disease-specific

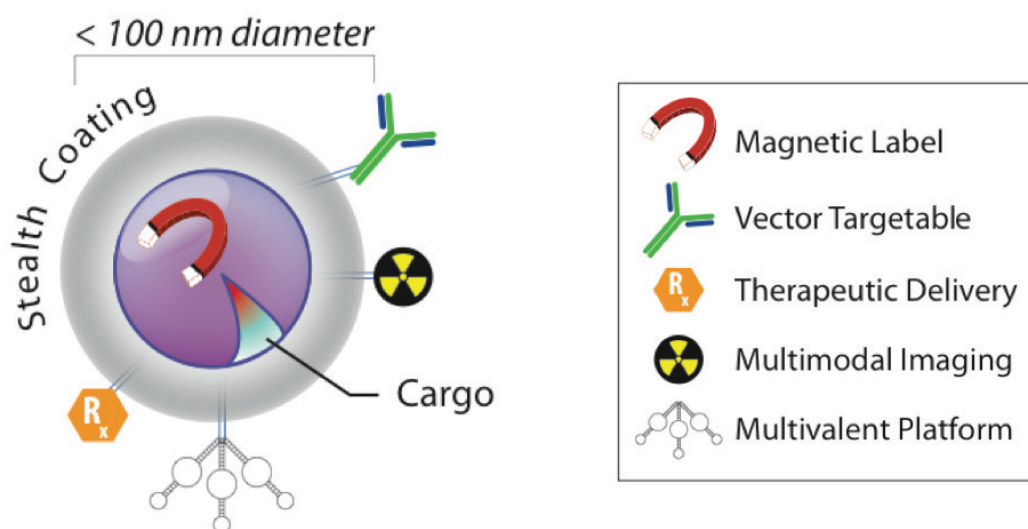


**FIG. 1:** Schematic of nanoparticle for imaging and therapy. Nanoparticles are structures generally described as being less than 100 nm in diameter that can be engineered to display specific chemical, physical, and biological properties. Working in biological environments often necessitates avoidance of the innate and adaptive immune systems often accomplished by polymer or polysaccharide coatings. Targeting of specific sites of disease can be accomplished with targeting moieties, including peptides, antibodies, and aptamers. Nanoparticles provide the opportunity to increase avidity for sites of interest through a strategy of multivalent attachment of a number of targeting ligands. This specific binding to sites of interest can then be exploited by the innate physical or chemical properties of the particle (e.g., quantum dots for fluorescence). Additionally, therapeutic chemicals or radioisotopes may also be conjugated to the particles.

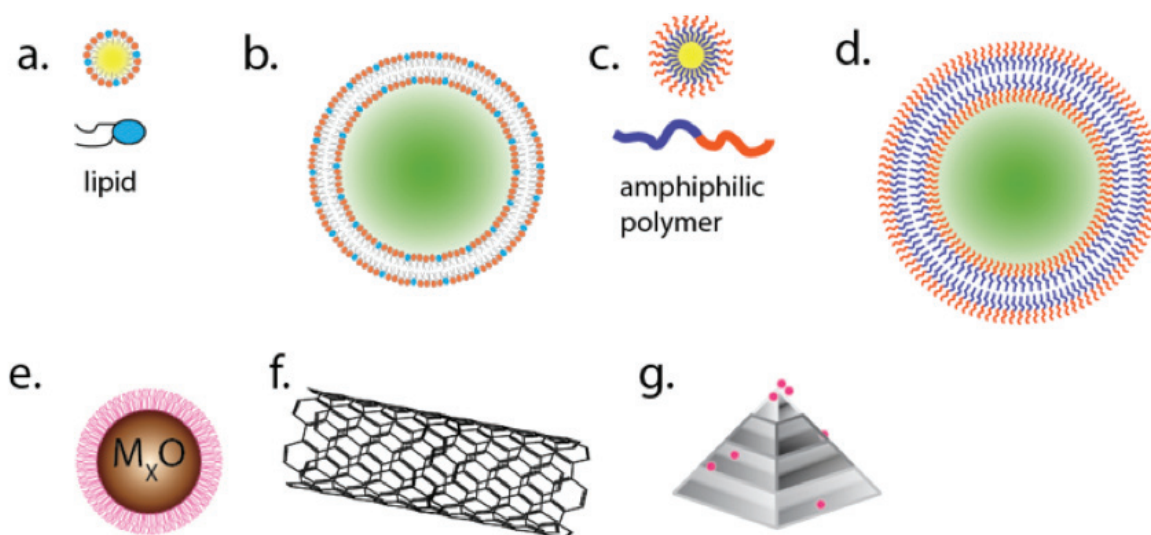


**FIG. 2:** Schematic representation of the diversity in nanoparticle architecture. A range of chemical and physical production strategies for nanoparticle synthesis results in different classes of particles. (a) Micelles and (b) liposomes are composed of either a single layer or bilayer of lipids, respectively. The interior of these structures can be used to deliver imaging or therapeutic agents. (c) Polymer micelles and (d) polymersomes exploit the same properties of amphiphilic molecules, but instead utilize man-made polymers for more stable, but usually larger, structures than liposomes. (e) Metal-based nanoparticles, usually passivated for biological applications with polymer, polysaccharide, or biological surface groups, have been made from an incredible number of different starting materials. Some of the most popular for imaging and therapy are iron oxides, gold, and silver. Carbon-based materials, such as (f) carbon nanotubes and (g) nanodiamonds, are of intense interest because of unique physical properties resulting from these highly structured nanomaterials.

imaging. Quantum dots (QDs) are semiconducting fluorescent NP with size-dependent optical properties; the emission wavelength of the particles can be tuned by adjusting the particle diameter.<sup>4</sup> Typically, the particle diameter is 1–8 nm.<sup>5</sup> Generally, QDs possess continuous absorption profiles that decrease in intensity up to their narrow emission lines. These narrow emission bands, and the greater photostability relative to small molecule organic dyes, have enabled the widespread use of the common CdS:ZnS QDs for *in vitro* microscopy applications.<sup>6,7</sup> Additionally, the larger multiphoton cross section of the NP relative to small molecules has been exploited for a range of applications, including deep-tissue intravital microscopy.<sup>8,9</sup> Use of these NP *in vivo* is primarily hampered by their toxicity due to the heavy metals contained within.<sup>10,11</sup> However *in vivo* investigations have demonstrated that nanoparticles are effective

agents for lymph node mapping,<sup>5,12</sup> which can be targeted by peptide or proteins toward disease-specific ligands.<sup>13–15</sup> Recent work has focused on the development of nonheavy metal biocompatible QDs.<sup>16,17</sup> Another approach to achieve bright, conjugatable fluorescent NP has been to encapsulate fluorescent small molecules either within or throughout a particle. An example of this technique is the core-shell silica NP (so called Cornell dots or C-dots), which is being introduced into the clinic. Particles in the single to 10s of nm range can be synthesized that incorporate covalently bound dye molecules.<sup>18,19</sup> The choice of dye determines the fluorescent emission, and particles have much greater brightness and photostability than single fluorescent moieties.<sup>18</sup> C-dots in the 6–10 nm range have been used for *in vivo* research, demonstrating high fluorescent output and rapid urinary excretion.<sup>20</sup> A multimodal radio-

iodinated ( $^{131}\text{I}$ ) derivative of this particle, functionalized with RGD to target  $\alpha_v\beta_3$  integrin on the tumor vasculature, has completed a phase 0 trial in man for technical feasibility.<sup>21</sup> Iron oxide NP for magnetic resonance imaging<sup>22</sup> and gold core nanoparticles (AuNP) for X-ray computed tomography<sup>23</sup> are among those that can be modified for fluorescence imaging. Since tissue attenuates any light and therefore both the excitation light and the emitted fluorescence, there is considerable interest in the use of the near-infrared (NIR) or even infrared wavelengths that can penetrate deeper into tissues.<sup>24,25</sup> Gold nanoparticles, as well as carbon-based materials (such as carbon nanotubes<sup>26,27</sup>), can be synthesized with emission wavelengths in the NIR region. Additionally, time-resolved fluorescence measurements could be used to decrease the autofluorescent background of tissue and cell samples. This has been used to great effect with QD and C-dot technologies,<sup>20,28</sup> as well as fluorescent nanodiamonds.<sup>29</sup>

### C. Surface-Enhanced Raman Spectroscopy

The Raman effect is an inelastic scattering event in which small numbers of incident photons' energy is decreased by the vibrational energy state of the scattering material. This phenomenon can be used for material and chemical analysis, but occurs at very low abundance. Materials have been designed that can greatly increase the likelihood of these events on a noble metal surface.<sup>30</sup> Silver and gold nanoparticles have been engineered to produce gains of Raman scattering >15 orders of magnitude that can be used *in vivo*. In their original work, Nie and Emory demonstrated single nanoparticle detection of the SERS effect for the rhodamine 6G-coated particles.<sup>31</sup> Integrin-targeting derivatives of these nanoparticles *in vivo* enabled the sensitive detection of tumors.<sup>32</sup> Many different particle categories have been used including lipid and silica-coated gold nanoparticles.<sup>33</sup> Recent efforts of SERS imaging have centered on multiplexed imaging (using multiple SERS sensitive dyes at the same time<sup>34</sup>) or multimodal imaging.<sup>35</sup>

### D. Photoacoustic Tomography (PAT)

Pulsed laser excitation into biological media results in local thermoelastic expansion of materials and structures that absorb that energy. When returning to lower ground state energy, the material shrinks. This high-frequency shrinking and expanding produces acoustic waves that can be used to detect fluorescent molecules using ultrasound-detecting equipment.<sup>36</sup> The major advantages of PAT techniques are greater spatial resolution at greater depths because the scattering of ultrasonic signals is many times less than that of light (i.e. fluorescence) *in vivo*. Many structures, such as melanin or hemoglobin, have wavelength-dependent absorption and PAT properties.<sup>37</sup> Exogenous probes in the form of nanoparticles have also been made for production of PAT signals. These primarily include fluorescent, carbon, or gold-based materials. QDs are most often used for their fluorescent emission properties, however, they also produce significant PAT signals.<sup>38</sup> Targeted agents including RGD-targeted CNT<sup>39</sup> and gold nanocages for targeted detection of melanoma,<sup>40</sup> as well as passive accumulation of AuNP,<sup>41</sup> produce significant PAT signals for disease detection. Overall, the combination of strong lasers for a deep tissue penetration and collection of the signal with ultrasound system could expand the depth in which fluorescent agents can be detected and could therefore be useful for further clinical explorations.<sup>42</sup>

### E. Magnetic Resonance Imaging with Nanoparticle Agents

In contrast to optical imaging modalities, magnetic resonance imaging (MRI) enables noninvasive deep tissue imaging of soft-tissue structures. The technique is based on the use of radiofrequency (RF) pulses that are used to manipulate the aligned magnetization of protons (primarily) of tissues placed in a strong external magnetic field. Currently, clinical MR scanners range in strength from 0.47 T to 7 T, with preclinical devices stretching into the 11.4 T range, but even higher field strengths are being explored. The inherent sensitivity of this imaging

modality is however quite low, since the majority of water's protons are not aligned in the direction of the applied field, and thus the distinction between adjacent tissues, or between sites of healthy and diseased tissues, is often difficult. To ameliorate this deficiency, magnetic contrast agents are often used. Most commonly applied in the clinic are gadolinium chelates. These small, linear or cyclic chelates are suboptimal in many cases since they clear rapidly, and their high rotational freedom does not allow for a very high relaxivity (a measure of the contrast generated per species). However, superparamagnetic nanoparticles are capable of generating significant contrast by affecting water protons' relaxation times, such as  $T_1$  (spin-lattice relaxation time, which is the time needed for the magnetization vector's  $M_z$  component to reach 63% of its original state following its 90 deg radiofrequency pulse flipping onto the transverse magnetic plane) and  $T_2$  (spin-spin relaxation, which is the time needed for the magnetization vector to recover 37% of its original status following an application of 90 deg and 180 deg radiofrequency pulses that cause displacement of the longitudinal magnetization onto the transverse plane). This section will cover  $T_1$ - and  $T_2$ -weighted MR nanoparticles, concentrating on the synthesis and characterization of iron oxide nanoparticles (IONPs) and their subsequent clinical translation. A brief review of the use of these agents for therapy will then be presented.

## F. Imaging with $T_1$ -Weighted MR Nanoparticles

For imaging, protons are excited by RF pulses. To come back to a lower energy ground state, the protons must pass their energy to the surrounding environment lattice. Longitudinal relaxation ( $T_1$ ) describes the time in which it takes a proton to become realigned with the applied magnetization direction. To enhance the contrast between tissues and tissue compartments (such as the blood or cerebrospinal fluid), it may be necessary to administer the chelated paramagnetic ion gadolinium. Enhanced contrast can be generated using NPs most simply by synthesis of

probes that bear multiple chelation sites for gadolinium. Such an approach has been accomplished with the most chemical rigor using dendrimer particles. Dendrimers of different generations (size and functional groups) have been generated with terminal gadolinium chelates as so-called gadomers.<sup>43</sup> The chelates are most commonly Gd(III)-N,N',N'',N'''-tetracarboxymethyl-1,4,7,10-tetraazacyclododecane (Gd(III)-DOTA) or Gd(III)-diethylenetriamine pentaacetic acid (Gd(III)-DTPA).<sup>44</sup> Increasing from the small molecular weight linear DTPA-Gd monomer to as many as 64 chelated Gd ions per particles results in an increase in both the per-Gd and per-agent relaxivity.<sup>45</sup> The ultimate result is a decrease in minimum detectable concentration of contrast. Targeted gadomer particles have been generated against the folate receptor,<sup>46,47</sup> as well as with a peptide against the transferrin receptor,<sup>48</sup> both overexpressed in many malignancies. Clusters of dendrimers conjugated together provide a larger free water exchange coefficient and further increase the rotational correlation time by increasing the molecular weight of the complex. These dendrimer nanoclusters have been synthesized and also used to target the folate receptor.<sup>49</sup> Retention of higher generation (larger molecular weight) gadomers in the liver has been cited as a potential problem. However, polyethylene glycol modification of the particles, for avoidance of the reticuloendothelial system, largely ameliorated this problem.<sup>50</sup> This issue of biodistribution of the toxic gadolinium ion at later times has not been further investigated for dendrimers. The cavities and surfaces of lipid and polymer-based vesicles have also been exploited for Gd chelation. These larger particles (often greater than 80 nm in diameter) can carry large payloads of the ion and have been investigated for several decades.<sup>51</sup> Refinements in production and labeling have resulted in liposome probes with increased signal characteristics.<sup>52</sup> Furthermore, polymer-based and hybrid lipid-polymer vesicle particles have been evaluated for greater stability<sup>53</sup> and improved targeting<sup>54</sup> and contrast.<sup>55</sup> Manganese-based NPs also produce positive  $T_1$  contrast.<sup>56</sup> These nanoparticles have been used in a range of applications, particularly to study cells and structures within the rodent brain.<sup>57,58</sup>

## G. Imaging of T<sub>2</sub>-Weighted MR Nanoparticles

T<sub>2</sub>-weighted imaging describes the dephasing, or loss, of transversely aligned spins. Inherent in imaging complex organisms is the presence of several magnetic heterogeneities generated by interfaces of different materials and fluids, which generates native T<sub>2</sub> contrast. This results in local signal hypointensity or negative contrast. Ameliorating this drawback is the fact that magnetic NP contrast agents can be engineered to provide passive or targeted local T<sub>2</sub>-weighted contrast to further dephase local spins. Currently, the most commonly used nanoparticles for MRI are iron oxide nanoparticles (IONPs) thanks to their generally benign profile<sup>59</sup> and uptake in a wide variety of cell types.<sup>60,61</sup> Multiple synthesis routes can be used to achieve nanoparticles <100 nm with varying magnetic, physical, and chemical properties (consolidated in a comprehensive review by Huber<sup>62</sup>). Usually, possessing a core of iron oxide (magnetite and/or maghemite) crystals surrounded by a polymer or polysaccharide coating, IONPs generate an intense T<sub>2</sub>-weighted signal. Other formulations, such as magnetodendrimers,<sup>63</sup> gold,<sup>64</sup> and silica-coated iron cores,<sup>65</sup> have also been investigated. The small iron oxide crystal core (<14 nm) imparts the property of superparamagnetism, and many IONPs are referred to as superparamagnetic iron oxides (SPIOs). These nanoparticles do not possess a permanent magnetism (unlike a ferromagnetic material, the classic magnet). In the presence of a strong magnetic field though, they align with the field and act as strong dephasing susceptibility agents. Without further modification, these nanoparticles are often quickly entrapped by the reticuloendothelial system and accumulate in the liver and spleen. Indeed, their first biomedical application was the identification of lesions by negative contrast.<sup>66,67</sup> Their cellular uptake, along with their biocompatibility (on degradation they enter the iron metabolism of the body), have led to the use of SPIOs for many preclinical cell tracking studies, including immune<sup>68,69</sup> and stem cells.<sup>70,71</sup> The use of large SPIOs enables detection down to the single-cell level,<sup>72</sup> and ultrasmall SPIOs have been used clinically.<sup>73</sup> IONPs can be modified for targeted

imaging with small molecules, peptides, antibodies, and aptamers. This can be achieved through a variety of conjugation methods: carbodiimide conjugation,<sup>74</sup> click chemistry,<sup>75</sup> and silane, among other approaches.<sup>76</sup>

## H. Nuclear Imaging and Nanotechnology

Nuclear imaging involves detecting radionuclides through emitted particles associated with their decay into more stable nuclides, which provides numerous advantages as an *in vivo* imaging modality. First, because the specific activity is often high for radiotracers, picomolar amounts of the radiotracer can be imaged, allowing non-pharmacologic doses that do not affect the biological system (commonly known the “radiotracer principle”).<sup>77</sup> Second, nuclear imaging is noninvasive and may be used serially over a time course to track a biological process, such as glucose metabolism.<sup>78</sup> Third, nuclear medicine images are quantitative, meaning that the image intensity corresponds to the concentration of radioactivity in an area.<sup>79</sup> In comparison to other common imaging modalities, such as MR and CT imaging, nuclear imaging offers superior sensitivity.<sup>80</sup>

Radioisotopes have been combined with various types of nanoparticle platforms for imaging. By conjugating multiple radionuclides to one platform, the specific activity, and therefore signal, delivered to a site of interest can be increased. Delivery of the radiolabeled nanoparticle to the site of interest can occur either by enhanced permeability and retention (EPR)<sup>81,82</sup> or through conjugating targeting ligands, such as small molecules,<sup>83</sup> peptides,<sup>84</sup> aptamers,<sup>85,86</sup> and antibodies<sup>87</sup> to the nanoparticle surface. An important consideration in radiolabeling nanoparticles is to match the kinetics and bio-distribution of the nanoparticle with the half-life of the radioisotope. A practical goal is to choose a radionuclide with a half-life short enough to limit patient exposure to ionizing radiation, but long enough that the radiolabeled entity can be clearly distinguished from the background. PET agents paired with nanoparticles include fluorine-18 (<sup>18</sup>F), copper-64 (<sup>64</sup>Cu), yttrium-86 (<sup>86</sup>Y), zirconium-89

( $^{89}\text{Zr}$ ), and iodine-124 ( $^{124}\text{I}$ ), while the SPECT tracers technetium-99m ( $^{99\text{m}}\text{Tc}$ ), indium-111 ( $^{111}\text{In}$ ), and rhenium-188 ( $^{188}\text{Re}$ ) have been combined with nanoparticles, among others.

Utilizing nanoparticles as platforms for radionuclides requires attaching the radionuclide to the nanoparticle. While certain nanoparticles such as liposomes and micelles can envelope the radionuclide,<sup>88</sup> other nanoparticles with metallic cores such as iron oxide nanoparticles (IONPs) and gold nanoparticles (AuNPs) require surface attachment. This is accomplished by conjugation of a chelator for metallic radioisotopes or a prosthetic group for nonmetallic radionuclides such as halides. Conjugation of chelators is accomplished through utilizing functional groups, such as amines and carboxyl groups on the nanoparticle coating.<sup>89,90</sup> Direct conjugation of radiohalides can occur via attachment of the radionuclide to a prosthetic group previously attached to the nanoparticle.<sup>91</sup>

## I. PET Imaging

PET Imaging involves detecting radionuclides that decay to a daughter isotope via the emission of a positron from the nucleus. In comparison to SPECT, PET offers superior sensitivity and spatial resolution,<sup>92</sup> making PET radiotracers attractive imaging agents. Combining the intrinsic sensitivity and quantitative aspects of PET imaging with the platform structure of nanoparticles has been the subject of intensive research for the past decade. Coupling MRI-active nanoparticles with PET tracers has attracted considerable interest as multimodal probes. These typically have a composition of an iron oxide or gadolinium containing nanoparticle with the radiotracer conjugated to the surface of the nanoparticle. MRI-active nanoparticles have been labeled with a plethora of PET tracers, such as  $^{18}\text{F}$ ,  $^{64}\text{Cu}$ , and  $^{89}\text{Zr}$ , depending on the blood clearance kinetics of the nanoparticle. Recently, iron oxide nanoparticles were radiolabeled with  $^{11}\text{C}$  using [ $^{11}\text{C}$ ] methyl iodide as a methylation agent. This was conjugated through both carboxylic acid and amino functional groups and the radiolabeled nanoparticle showed liver accumulation

in an *in vivo* mouse model, but the short half-life of  $^{11}\text{C}$  ( $t_{1/2} = 20.3$  min) requires nanoparticles that have rapid kinetics.<sup>93</sup> A hetero-nanostructure of gold and iron oxide was developed as a multimodal probe. After synthesis, the nanoparticle was labeled with  $^{64}\text{Cu}$  along with an anti-EGFR antibody, and imaged with PET, MRI, and optical modalities.<sup>94</sup> Furthermore, single-walled carbon nanotubes (SWCNTs) have pharmacokinetic profiles that offer rapid blood clearance, making shorter-lived radionuclides attractive for labeling.<sup>95</sup> SWCNTs were radiolabeled with  $^{86}\text{Y}$ , with whole-body PET, indicating major sites of accumulation in the kidneys, liver, and spleen in an athymic nude mouse model.<sup>96</sup>

Liposomes are another class of nanomaterials used for PET imaging, which allow molecules, including radionuclides, to be enclosed within. By using the hydrophobic pockets of the liposome,  $^{89}\text{Zr}$  was encompassed in a liposome containing also [Gd]-DTPA, using a chelator-free method, which was then labeled with octreotide to target human somatostatin receptor subtype 2 (SSTR2). This PET/MR active liposome showed approximately twofold tumor uptake of the targeted nanoparticles (3.5–5.0%ID/g) compared to non-targeted controls (2.5–3%ID/g) at 50 h postinjection a xenograft mouse model, but higher bone uptake (12%ID/g) compared to chelated zirconium nanoparticles was a limitation observed using this method.<sup>88</sup>  $^{64}\text{Cu}$  was used to radiolabel 120 nm diameter liposomes, which had greater uptake in the tumor compared to FDG uptake in a murine model of mammary carcinoma.<sup>97</sup> Quantum dot micelles composed of phospholipids were labeled with  $^{18}\text{F}$  for *in vivo* multimodal imaging and showed a circulation half-time of 2 h.<sup>98</sup> Whereas previous polymer-coated nanoparticles were taken up within minutes by the RES system,<sup>99</sup> the longer half-life of the phospholipid nanoparticles allows for biomarker specific targeting to take place. Micelles conjugated with anti-CD105 monoclonal antibody were radiolabeled with  $^{64}\text{Cu}$ , loaded with doxorubicin, and exhibited pH-sensitive drug release, with a blood half-life of several hours.<sup>100</sup>

## J. SPECT Imaging

SPECT imaging utilizes nuclides that decay via the emission of single gamma rays with differing energies depending on the radionuclide. A collimator detects these photons, and the image is reconstructed. However, because of the necessity of a collimator, the sensitivity of SPECT is several orders of magnitude lower than PET and it is so far not yet quantitative in nature.<sup>101</sup> However, many SPECT radionuclides, such as <sup>99m</sup>Tc, are eluted from a generator, alleviating the need of an on-site cyclotron. Additionally, while having inferior sensitivity and resolution compared to PET, SPECT does have the benefit of allowing simultaneous imaging of multiple isotopes,<sup>102</sup> as well as longer radionuclide half-lives and potentially higher resolution. For dual modality MRI/SPECT agents, magnetic nanoparticles have been labeled with SPECT radionuclides. Bisphosphonate was used to anchor PEG to an iron oxide nanoparticle, which was subsequently radiolabeled with <sup>99m</sup>Tc.<sup>103</sup> These nanoparticles showed a blood half-life of 3 h with low reticuloendothelial system uptake. <sup>99m</sup>Tc was also used to label polymer-shelled microbubbles of superparamagnetic iron oxide nanoparticles (SPIONs) that were functionalized with NOTA or DTPA. The biodistribution of the microbubbles showed a dependence on the chelator used, with generally high uptake for each system seen in the liver, spleen, and kidneys at 24 h.<sup>104</sup> Alternatively, doxorubicin-loaded liposomes capable of MR, NIR, and nuclear imaging were generated and injected intratumorally in squamous cell carcinoma of head and neck tumor xenografts. These liposomes were radiolabeled with <sup>99m</sup>Tc for SPECT imaging or <sup>64</sup>Cu for PET, but no systemic injections were reported.<sup>105</sup> <sup>188</sup>Re liposomes were generated and tested *in vivo* in a C26 colonic peritoneal carcinomatosis mouse model. The nanoparticles accumulated via the EPR effect and showed 7.91% injected dose per gram in the tumor at 24 h, with a tumor-to-muscle ratio of 25.8. <sup>188</sup>Re-labeled PEG-ylated liposomes were generated and evaluated in a glioma mouse model, and showed a 1.95% injected dose per gram in the tumor at 24 h, with a 32.5 tumor-to-brain ratio.<sup>106</sup> Similarly, a micelle with a GRP78 binding peptide

was generated for a gastric xenograft model. The micelles were radiolabeled with <sup>111</sup>In conjugated with DTPA, and *in vivo* tests with the GRP78BP micelle showed higher uptake compared to a non-targeted control.<sup>107</sup> Multifunctional micelles were generated that contained both a near-infrared dye IR-780 and <sup>188</sup>Re, allowing imaging by both NIR fluorescence and SPECT. Additionally, the dye allowed photothermal therapy *in vivo* with histopathology showing irreversible tissue damage after *in vivo* photothermal ablation.<sup>108</sup>

## II. WHAT SHALL THE FUTURE BRING IN NANOTECHNOLOGY-BASED NUCLEAR IMAGING?

A number of recent innovative publications show novel ways for improved imaging and therapy through combining nanoparticles with radionuclides. With the advent of bioorthogonal click chemistry,<sup>109</sup> new methods of imaging and therapy with radionuclides are in development. Although pre-targeting with an antibody-PET tracer system has recently been accomplished using the transcyclooctene/tetrazine system,<sup>110</sup> an analogous strategy using pre-targeting with antibodies and nanoparticles could feasibly allow less ionizing radiation dose to the RES while still obtaining high specific activity.<sup>111</sup> Raman-active particles have become increasingly popular since they offer exquisite signal-to-background levels, but the Raman signal is quickly quenched at depths of a few millimeters.<sup>35</sup> Radiolabeling Raman-active particles allows the particles to be noninvasively imaged regardless of depth,<sup>112</sup> while the highly specific Raman signal at the surface allows for intraoperative imaging for surgical assistance.<sup>113</sup> By combining these modalities, a one-shop system could conceivably be used for both preoperative and intraoperative imaging.

Because of the “always-on” nature of radionuclides, measuring a functional response with radionuclides has not been possible until recently. Cerenkov light from [<sup>18</sup>F]-FDG was used to excite a fluorescent probe that was delivered to tumors via conjugation to gold nanoparticles.<sup>13</sup> The nanoparticles contained a fluorescein bearing peptide that when bound to



the gold nanoparticle was quenched. The peptide was cleaved by MMP-2, which is overexpressed in many more aggressive cancers, causing the release of FAM, which was then excited by Cerenkov from [ $^{18}\text{F}$ ]-FDG. Another report of Cerenkov imaging with a nanoparticle system involved gold nanocages, which were recently synthesized with  $^{198}\text{Au}$  being incorporated within the Ag nanocubes by galvanic replacement reaction (Fig. 3).<sup>114</sup> After PEGylation of the 35 nm nanocubes, the particles showed a high tumor-to-muscle ratio at 24 h, with a clear delineation of the tumor by Cerenkov imaging.

## A. Nanotechnology in Cancer Therapy

### 1. From Conventional Chemotherapeutics to Advanced Treatment

Cancer is among the leading causes of death in the world, with more than a million new cases each year in the United States and several hundred thousand deaths.<sup>115</sup> Apart from substantial mortality, cancer has major economic impact due to the associated health-care costs for diagnosis, treatment, and management. Advancements in cancer biology allowed deciphering how cells can become malignant and why effective cancer treatment stills remains a challenging conundrum.<sup>116</sup> Although surgery and radiotherapy have been widely used for decades, advanced chemotherapeutics gradually reach the clinic, in

order to achieve tumor regression via inhibition of fundamental cellular processes, such as cell division and metabolism, or blocking of overactive signaling pathways. The primary challenge that these drugs face is their ability to reach the lesion at adequate concentrations, and once in the cell's vicinity to associate with their target and eventually initiate cell death. From the time that a drug enters a patient's body, it constantly encounters barriers and clearance mechanisms that can quickly eliminate it, including serum proteins, immune cells, and excretory organs. Hence having drug delivery systems that will improve cancer chemotherapeutics' time in circulation, protect them from degradation, and release them only at the site of disease to reduce side effects is critical and would improve efficacy.<sup>117-119</sup>

Supramolecular drug delivery systems, including nanoparticles, had already been proposed in the late 1970s, as tunable platforms that can enhance drug's efficacy by improving their target cell uptake and achieving controlled drug release within an optimal range of therapeutic concentration.<sup>120</sup> Since the cost and time for the development of a new drug delivery system are lower than those for the development of a new drug (\$50 million in four years versus more than \$500M in 10 years), the health-care industry encourages the introduction of advanced delivery systems.<sup>121</sup> An indicator of this trend is the growth of the U.S. drug delivery system market, which has expanded from \$75 million in 2000 to \$121 billion in 2010.<sup>122</sup> Similarly, the allocation of research funds has

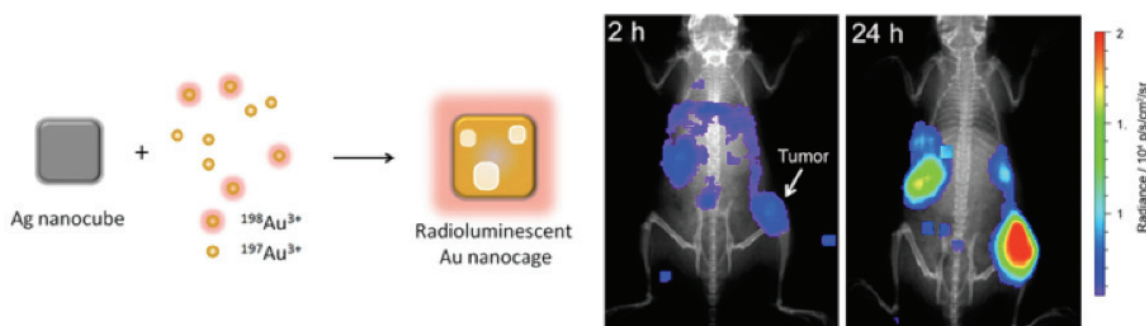


**FIG. 3:** Construction of a radioluminescent nanocage using silver nanocubes and gold radionuclides. Enhanced tumor uptake was observed after 24 h, based on Cerenkov imaging. Adapted with permission from Ref. 114. Copyright 2013 American Chemical Society.

substantially increased, where U.S. government funding agencies provided more than one billion dollars for the investigation of nanotechnology-based drug delivery platforms in the last 10 years.<sup>118</sup> Research has provided us with novel nanomaterials with unique architectures and capabilities, which demonstrate cancer selectivity, improved pharmacokinetics and enhanced cytotoxicity. FDA-approved drug delivery systems that are currently in the clinic for the treatment of different cancers or infections include lipid-based and polymeric nanoparticles indicative of the exciting new era in nanotechnology-based cancer chemotherapy.

What makes nanoparticles attractive drug delivery vehicles is their ability to have tunable properties, such as size, shape, surface charge, valency, and compartments.<sup>117,118,123–125</sup> Particularly, size is of major importance during synthesis, because nanoparticles of the same material and different size can have different toxicity, uptake, and fate within the cell.<sup>126–128</sup> Furthermore, size plays a role in the way that the nanoparticles are recognized by the immune system and how the nanoparticles will be cleared from the body.<sup>129,130</sup> Likewise, the shape of the nanoparticles is a key factor in how these agents will interact with the cells. For instance, spherical or rodlike nanoparticles aligned perpendicular to the plasma membrane will be more effectively uptaken by the cell, while elongated wormlike nanoparticles avoid phagocytosis.<sup>131,132</sup> Long carbon nanotubes with diameter of a few nanometers can be rapidly uptaken by the cells, yet they are surprisingly quickly removed from the body through renal clearance.<sup>133</sup> Perhaps the most common approach to improve the aqueous stability and circulation times of nanoparticles is the conjugation of polyethylene glycol (PEG) groups to the nanoparticles' surface.<sup>134,135</sup> Apart from decreasing immunogenicity and preventing activation of the complement cascade, the pegylation of nanomaterials lowers opsonization and nonspecific uptake by the reticuloendothelial system.

Paradoxically, although nanoparticles have to avoid nonspecific uptake and either renal or hepatic clearance, they also have to release their therapeutic payload at the tumor, in order to minimize systemic toxicity and maximize the drug's

local concentration at the pathology. In general, most primary solid tumors have a leaky vasculature, which allows retention of nanoparticles between 30 and 200 nm via the enhanced permeability and retention effect.<sup>118,136</sup> Hence, this passive targeting allows the nanoparticles to be sequestered within the tumor, and release the drugs on encountering unique conditions at the tumor's environment, such as enzymes and pH. An attractive element of this approach is that the drug delivery vehicle does not undergo any extensive modification, which might be desirable for fast regulatory approval. Since tumor heterogeneity might result in nonuniform vascularization and vessel permeability, it is possible for different areas in the lesion to variably retain the nanoparticles and induce drug resistance.<sup>137,138</sup> Alternatively, active targeting may be utilized where the nanoparticles are conjugated with affinity ligands, whose receptors are overexpressed on the cancer cell's plasma membrane or are in abundance within the tumor's microstructure. From antibodies to their fragments, and from aptamers to peptides and small molecules,<sup>118</sup> the library of tumor-targeting moieties continuously expands, as researchers identify new molecular landmarks and biomarkers on tumors. Conjugation of these ligands to the nanoparticle surface is achieved through facile chemistries, such as carboxyl-to-amine (EDC) or propargyl-to-azide ("click"), that allow the formation of stable covalent bonds. The density of receptors at cancer cells' plasma membrane is important for the nanoparticle uptake, allowing multiple interactions between the cells and the drug delivery vehicles. In the case of ErbB2-targeting liposomes that carried Doxorubicin, the high levels of ErbB2 were important in the uptake of the nanoparticles and intracellular release of the drug.<sup>139</sup> Furthermore, meticulous grafting of the nanoparticle surface with targeting ligands can render the nanoparticles multivalent agents and confer improved drug delivery, due to the enhanced binding of the nanoparticle with receptors at the target cell.

## 2. Polymeric Nanoparticles

Among the most versatile platforms for drug delivery are polymeric nanoparticles, which have significantly evolved since the 1970s.<sup>140</sup> Initial attempts included the conjugation of drugs to polymers, in an effort to substantially increase their molecular weight and avoid rapid renal clearance.<sup>141,142</sup> Many drugs, including paclitaxel, doxorubicin, and camptothecin, were conjugated to poly(L-glutamic acid) (PGA) and *N*-(2-hydroxypropyl) methacrylamide (HPMA) among other polymers.<sup>143,144</sup> In addition to improved bioavailability, HPMA was utilized as a multifunctional platform for drug delivery and imaging, where the polymer was conjugated to radiolabeled cyclical RGD peptide.<sup>145,146</sup> However, several drug-polymer conjugates were associated with side effects and unpredictable drug release that slowed their approval by regulatory agencies, priming the emergence of polymeric nanostructures as drug delivery vehicles.<sup>147</sup> Hence, contemporary polymeric nanoparticles have been engineered to provide multiple attractive properties. For instance, apart from demonstrating improved *in vivo* stability, they are biodegradable, with tunable degradation rates, and concomitantly controllable drug release. Poly(lactic acid) (PLA), poly(glycolic acid) (PGA), and their copolymer poly(lactic-co-glycolic acid) (PLGA) have been used for the delivery of small molecules, peptides, proteins, and DNA.<sup>148–150</sup> Since PLGA can be easily processed, investigators were able to tune the size of nanoparticles through innovative fabrication protocols. Likewise, judicious selection of PLGA's monomeric subunits can enhance the nanoparticles' characteristics. It was demonstrated that the nanoparticles' drug release rate was affected by changing PLA's molecular weight while the D-PLA enantiomer forms nanoparticles with enhanced mechanical properties.<sup>151,152</sup> Additional hybrid polymeric drug delivery vehicles have been developed, in order to target multiple oncogenic mechanisms, such as angiogenesis and aberrant cell division. In an elegant study, PLGA nanoparticles carrying doxorubicin where coated with a PEGylated lipid that entrapped the anti-angiogenic drug combretastatin.<sup>153</sup> On retention of the nanoparticles in the tumor and degradation of the nanoparticles'

lipid coating, combretastatin was released, causing disruption of the tumor neovasculature and reduction in blood supply. As a result, the doxorubicin-loaded PLGA nanoparticles were entrapped within the tumor, and readily internalized by cancer cells, leading to tumor regression. With the development of new classes of chemotherapeutics, such as photosensitizers that become highly cytotoxic on light irradiation, Weissleder and colleagues have used PLGA as a drug delivery vehicle of meso-tetraphenylporphyrin.<sup>154</sup> The nanoparticles were able to release the photosensitizer *in vitro* and *in vivo*, and topical irradiation with visible light achieved complete tumor regression in mice [Fig. 4(a)]. This hints at the potential use of this approach in laparoscopic and endoscopic therapeutic interventions with low systemic toxicity. In an effort to make PLGA nanoparticles specific toward a tumor, researchers have conjugated targeting moieties to these nanoparticles, in order to associate with the prostate-specific membrane antigen that is overexpressed in prostate cancer and the neovasculature of the majority of solid tumors.<sup>155</sup> These docetaxel-carrying nanoparticles had a blood half-life of 20 h with low liver accumulation, and were able to gradually release their content, achieving 100-fold higher drug plasma concentration than the free drug and enhanced tumor reduction [Fig. 4(b)].

Other polymeric vehicles have been developed and approved by the FDA, including polyanhydrides, which degrade on hydrolysis of the anhydride linkage.<sup>147</sup> One of them, the polyanhydride wafer Gliadel has been approved for the treatment of patients with malignant glioma to complement surgery and radiation.<sup>156</sup> Advancements in the field include the introduction of block copolymers, such as a poly(propylene oxide)-poly(ethylene oxide)-poly(propylene oxide) (PEO-PPO-PEO) and a modified poly(aspartic acid) linked to PEG.<sup>157,158</sup> These polymers are in clinical trials in the United States and abroad for the delivery of doxorubicin and paclitaxel.<sup>147</sup> Meanwhile, research efforts have been focused on improving polymeric nanoparticles' stability, such as by enhancing the hydrophobicity of the nanoparticle cavity through introduction of hydrophobic moieties to the polymer, increasing the cavity's capability to form multiple hydrogen bonds and electrostatic associations, and

cross-linking the cavity. Adopting these principles, Santra *et al.* created a hyperbranched polyester from diethyl malonate, which allowed the formation of highly stable nanoparticles that had a hydrophobic core and surface functional groups.<sup>159</sup> Due to the polymer's stability, the corona's carboxylic acid groups were easily converted to amine, propargyl, or azide, which allowed the conjugation of targeting moieties, such as folic acid. The resulting nanoparticles successfully co-delivered paclitaxel and the fluorophore DiI to folate-receptor-expressing cancer cells, where the nanoparticles gradually released their cargo on degradation in the acidified late endosomes and lysosomes. Additionally, two different populations of hyperbranched polymeric nanoparticles were chemically linked to each other, yielding nanocomposites with drug delivery, imaging, radio-protecting, and magnetic capabilities [Fig. 4(c)]. Hyperbranched polyester nanoparticles were also used for the *in vivo* delivery of the cytotoxic peptide CT20p, due to its unique amino acid composition.<sup>160</sup> This peptide derived from the pro-apoptotic effector Bax, and includes hydrophobic and cationic amino acids on its sequence, which allow CT20p to bind to the mitochondrial membrane and initiate apoptosis. Intriguingly, delivery of the peptide with the nanoparticles achieved remarkable tumor regression [Fig. 4(d)], through an alternative mechanism that did not exclusively rely on effector caspases and was unaffected by overexpression of the anti-apoptotic protein Bcl-2. Others used polymeric nanoparticles for the co-delivery of paclitaxel and siRNA to inhibit the expression of the oncogenic serine/threonine-protein kinase PLK1 and accomplish a synergistic therapeutic effect.<sup>161</sup> Although most chemotherapeutics are hydrophobic, therapeutic proteins and endogenous cytotoxic agents, such as the cytochrome c that initiates the apoptotic cascade, are hydrophilic. Delivery of cytochrome c to cancer cells was achieved through encapsulation of the protein within hyperbranched polyhydroxyl nanoparticles, which preserved cytochrome's structure and enzymatic activity, eventually leading to significant cell death in targeted cells.<sup>162</sup>

Since nature widely employs polymers made from simple precursors such as carbohydrates, nucleic acids, and amino acids, researchers have used natural

polymers, due to their biocompatibility and pharmacokinetics. Polysaccharides, such as chitosan, have been used for the delivery of chemotherapeutics, yet toxicity issues have to be addressed depending on the polymer used.<sup>163</sup> Polymeric nanoparticles with carbohydrate units and glycosidic bonds that are found within the human body are attractive alternatives, due to their lower toxicity and immunogenicity. In a recent study, polymeric nanoparticles made from glucosamine-conjugated poly(isobutylene maleic acid) and loaded with cisplatin achieved tumor reduction in breast, lung, and ovarian cancer models.<sup>164</sup> Other groups utilized DNA and RNA's unique interactions to form supramolecular structures for the delivery of doxorubicin, methylated oligonucleotides, and siRNA.<sup>165–167</sup> With the evolution of DNA origami, DNA nanotubes, nanoboxes, and nanorobots were developed.<sup>168–170</sup> In fascinating studies, DNA nanorobots were able to process inputs based on logical gates that served as environmental antigen keys capable of activating the nanobots.<sup>171</sup> These nanobots controlled cell signaling by releasing antibodies and antibody fragments that targeted CD33 and CDw328 in aggressive NK leukemic cells. The nanorobots inhibited cell cycle progression, as well as the phosphorylation of the Jun N-terminal kinase (JNK) and Akt. Potentially, the *in vitro* and *in vivo* stability of DNA nanoparticles can be further enhanced with the use of modified nucleic acids, which can preserve the nanoparticles from early nuclease degradation.

Elegant nanostructures can be created from amino acid building blocks, conferring properties such as biocompatibility, targetability, and low antigenicity.<sup>147</sup> Elastomer-like and silklike proteins have been utilized for drug delivery, since their molecular weight, hydrophobicity, and bioconjugation sites can be judiciously engineered. Elastin-like proteins have the amino acid sequence GVGVP as their building block, whereas silklike proteins have alternate repeats of glycine and alanine.<sup>172,173</sup> Drug and gene delivery have been accomplished, and recent studies revealed that these protein-based polymers might serve as high avidity drug delivery platforms, due to the multiple interactions between targeting moieties and cells.

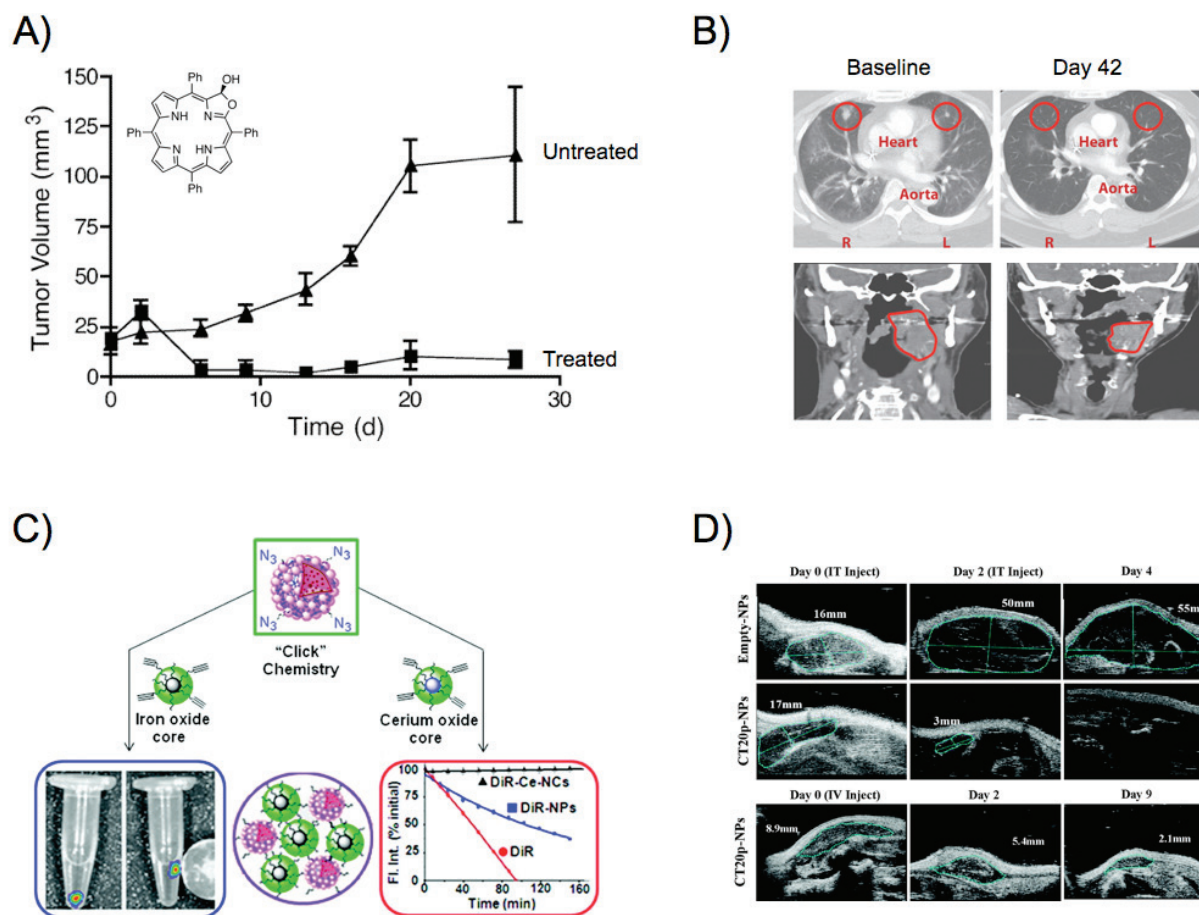


**FIG. 4:** Polymeric nanoparticles in cancer therapy. (a) PLGA nanoparticles delivered meso-tetraphenylporpholactol to prostate cancer xenografts in mice. Treatment of tumors with light resulted in tumor regression due to activation of the phototoxic agent, while the untreated tumors (no light treatment) continued growing. Adapted with permission from Ref. 154. Copyright 2005 American Chemical Society. (b) Axial contrast-enhanced CT scans of a cholangiocarcinoma patient with lung metastases and coronal images of a tonsillar cancer patient before and after treatment with docetaxel-carrying targeted nanoparticles. Adapted with permission from Ref. 155. Copyright 2012 American Association for the Advancement of Science. (c) Composite nanomaterials with unique properties, courtesy of their magnetic and radiation-protecting nanoparticle building blocks. Adapted with permission from Ref. 159. Copyright 2010 American Chemical Society. (d) Intratumoral or intravenous administration of a cytotoxic peptide with polymeric nanoparticles results in tumor regression. Adapted with permission from Ref. 160. Copyright 2012 American Chemical Society.

### 3. Liposomes and Micelles

Another nature-inspired approach to deliver therapeutics to cells was introduced in 1965 by Alec Bangham using phospholipids,<sup>174</sup> which was later refined by Gregory Gregoriadis in the form of lipid-based drug delivery vesicles capable of retain-

ing drugs within them.<sup>175</sup> It was envisioned that this drug delivery platform could be biocompatible and biodegradable, as well as capable of delivering hydrophobic and hydrophilic therapeutics. Liposomes are spherical nanoparticles that have a phospholipid bilayer similar to mammalian cells, with an aqueous phase that can accommodate agents

with amphiphilic properties.<sup>176</sup> On the other hand, micelles are spheres that contain a lipid monolayer with the phospholipids' hydrophilic groups exposed to the aquatic milieu, forming a hydrophobic cavity. These structural differences between liposomes and micelles could be used for the retention of drugs with different characteristics, such as hydrophobicity and molecular weight. Particularly in the case of liposomes, extremely hydrophobic chemotherapeutics, like paclitaxel, cannot be efficiently retained within the liposomal vesicle, because the phospholipid bilayer is highly permeable to hydrophobic agents, as opposed to hydrophilic molecules that are confined within the liposomal cavity via multiple electrostatic interactions.<sup>177</sup>

Since fluorescent small molecules also have the ability to produce local chemical or direct thermal damage, with the potential for therapy, this strategy has resulted in several approved photodynamic therapy (PDT) approaches in the clinic.<sup>178</sup> Porphyrin-based PDT agents are notably difficult to solubilize and when systemically administered have the problem of possibly severe skin reactions (necessitating patients to avoid exposure to sunlight). Apart from porphyrins, methylene blue has some photosensitizer function, and nanoparticle encapsulated versions have been demonstrated to have cytotoxic effect.<sup>179</sup> Of particular interest is the new class of nanomaterial that was developed specifically for optical-based therapy and imaging called porphyrinsomes. Composed of bilayers of porphyrin-capped carbon chains, these 100 nm diameter structures are biodegradable, and strongly photothermal under NIR excitation.<sup>180</sup> Investigations have demonstrated that these nanoparticles are effective in hypoxic tumors, overcoming one known barrier to traditional effective treatment of tumors.

Although drugs can be stably accommodated within liposomes and micelles, drug delivery with these vehicles has been challenging, due to the nanoparticles' clearance through the reticuloendothelial system, enzymatic degradation by esterases and lipases at the liver, and structural instability of the nanoparticles that leads to vehicle aggregation or abrupt release of the therapeutic cargo.<sup>181</sup> Efforts to alleviate these problems include incorporation of cholesterol and sphingomyelin to restrict the fluidity

of the lipid bilayer and introduction of polyethylene glycol moieties.<sup>182,183</sup> For instance, the FDA-approved liposomal formulation Doxil consists of PEGylated liposomes loaded with doxorubicin, whereas the non-PEGylated liposomes daunorubicin-carrying DaunoXome and doxorubicin-encapsulating Myocet are used in the clinic to minimize the cardiotoxicity associated with the conventional delivery of the drugs that lack a delivery vehicle. To achieve specific drug delivery, peptides, glycoproteins, and antibodies were introduced to liposomes, where the presence of PEG within the lipid bilayer lowered steric hindrance and facilitated the conjugation of multiple targeting moieties.<sup>184–186</sup> The  $\alpha_v\beta_3$  integrin, which plays a key role in angiogenesis, was targeted with small cyclical RGD peptides that were introduced to both liposomes and micelles.<sup>187,188</sup> Clinical trials with an oxaliplatin-encapsulating transferrin-PEG and doxorubicin-carrying anti-ErbB2 liposomes demonstrated the translational potential of these systems, and how researchers creatively solved the initial targetability problems of liposomes.<sup>189,190</sup> Several other cancer biomarkers were utilized for the targeting of liposomes and micelles with monoclonal antibodies and antibody fragments, including the VEGFR2, EGFR, and EpCAM among others.<sup>191–193</sup> Likewise, with the identification of new therapeutics, liposomes were utilized for the delivery of antisense oligonucleotides and siRNA,<sup>194</sup> while novel drug release approaches for lipid-based carriers were developed, including hyperthermia, ultrasound, pH-sensitive linkages, and enzymes.<sup>195–198</sup>

#### 4. Metallic Nanoparticles

At the beginning of the twenty-first century, research efforts focused on the development of multifunctional nanoparticles, which can serve as drug delivery vehicles, therapeutic intervention mediators, and diagnostic or imaging agents. Iron oxide and gold nanoparticles have been extensively investigated in cancer therapy, due to their optical, magnetic, and photothermal properties. Multiple synthetic strategies yielded nanoparticles with different geometries, but almost all converge to the formation of polymer- or

small-molecule-stabilized nanoparticles.<sup>199</sup> Apart from providing aqueous stability and minimizing aggregation, the surface coating allows the conjugation of targeting moieties through facile chemistries, and the addition of polyethylene glycol moieties to minimize nonspecific uptake *in vivo*. Polymer-coated iron oxide nanoparticles, which carried doxorubicin, targeted the folate receptor via folic acid moieties found on the nanoparticles' coating.<sup>200</sup> These nanoparticles demonstrated enhanced tumor regression in folate-receptor-positive tumors, and were more effective than liposomal doxorubicin. Histochemical analyses revealed that the drug-loaded iron oxide nanoparticles more effectively reduced the expression of angiogenic biomarkers and increased apoptosis. The nanoparticles' localization was determined through MRI, and marked signal differences were observed in the folate-receptor-expressing tumors. Furthermore, strong magnetic fields can be used to increase the accumulation of the magnetic drug-loaded nanoparticle at known sites of disease.<sup>201,202</sup> One can also use an alternating magnetic field to locally heat the local environment of magnetic nanoparticles. The principle here is that energy is lost during the magnetization reversal process experienced by the nanoparticle within an alternating field (a difference in the hysteresis loop, friction, and magnetic effects). This energy, in the form of heat, is deposited by the nanoparticle in the local environment to a level lethal to cells.<sup>203</sup> Several superparamagnetic iron oxide nanoparticle formulations of varying size have been used for a range of cancer types in several small animal models of disease, including treatment of breast cancers,<sup>204</sup> prostate cancer,<sup>205</sup> and gliomas.<sup>206</sup> While not a commonplace practice for cancer treatment in patients, trials have evaluated the effects of local heating in the clinic (up to 49.5°C).<sup>207,208</sup>

Recent studies have yielded multimodal iron oxide nanoparticles, which allow imaging through magnetic resonance and fluorescence techniques. This was accomplished through the encapsulation of near-infrared lipophilic fluorophores within the cavities of poly(acrylic acid), which was utilized to stabilize iron oxide nanoparticles.<sup>209</sup> These dual MRI/fluorescent nanoparticles specifically delivered paclitaxel to folate-receptor-expressing cells, since

the carboxylic acid groups of the polymer were used for the conjugation of folic acid. Interestingly, the nanoparticles released their cargo within the cell's late endosomes and lysosomes, as the polymeric coating underwent degradation by enzymes and acid-mediated hydrolysis ( $\text{pH} \leq 4.5$ ) [Fig. 5(a)]. Similarly, cisplatin was released from ErbB2-targeting porous hollow iron oxide nanoparticles at low pH, on etching of the nanoparticle pores by the acidified milieu.<sup>210</sup> Magnetic-field-directed drug delivery was also accomplished with mesoporous silica-coated iron oxide nanoparticles, which in the presence of magnetic field significantly improved doxorubicin's delivery to tumors.<sup>211</sup> In an effort to achieve higher drug delivery and improved MRI signal, investigators loaded doxorubicin and iron oxide nanoparticles within a micelle's cavity.<sup>212</sup> The micelle targeted  $\alpha_v\beta_3$  integrin through cyclical RGD peptides, efficiently tracking  $\alpha_v\beta_3$ -positive cells and inducing cytotoxicity.

Improved drug efficacy was also observed with gold nanoparticles that were covalently linked to paclitaxel with DNA linkers.<sup>213</sup> This approach improved paclitaxel's solubility, and allowed the conjugation of many drug molecules with diverse linkers, ultimately making the nanoparticles potent chemotherapeutic systems. Alternatively, hydrophobic drugs were non-covalently retained within the interior of monolayers of gold nanoparticles, which were efficiently delivered within cancer cells.<sup>214</sup> In the case of photodynamic therapy, PEGylated gold nanoparticles delivered silicon phthalocyanine 4 *in vitro* and *in vivo*,<sup>215</sup> demonstrating that inorganic nanoparticles could be used to deliver prodrugs that are subsequently activated or released in the presence of stimuli, including light, temperature, acidity, hydrophobicity, and enzymes.<sup>214,216–220</sup> For instance, gold nanocages consisting of porous walls and hollow interiors were able to release their cargo, once they were illuminated with near-infrared light.<sup>221</sup> Gold nanoparticles were used for the photothermal ablation of melanoma, using nanoparticles that displayed a melanocyte-stimulating hormone analog on their surface.<sup>222</sup> Also exploiting the compromised plasma membrane as a result of topical heating during photothermal therapy with gold nanospheres, researchers accomplished improved *in vivo* delivery of drugs

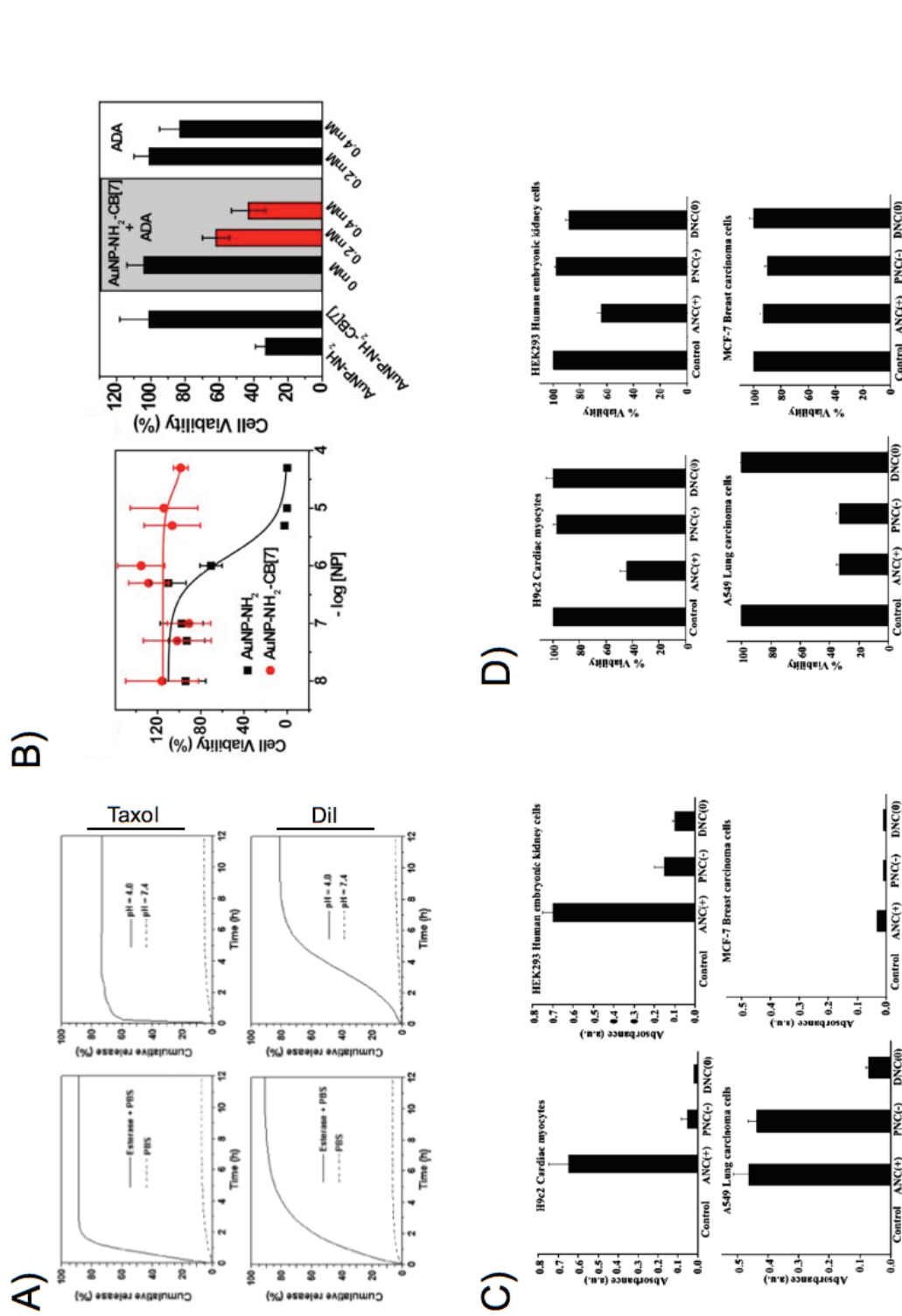


**FIG. 5:** (a) Poly(acrylic acid)-coated iron oxide nanoparticles loaded with Taxol and the fluorophore DiI release their cargo in the presence of esterase and acidic pH. Adapted with permission from Ref. 209. Copyright 2009 Wiley-VCH Verlag GmbH&Co. (b) *In vitro* removal of the cucurbit[7]uril cap from cationic gold nanoparticles in the presence of 1-adamantylamine renders them potent cytotoxic agents. Adapted with permission from Ref. 226. Copyright 2010 Nature Publishing Group. (c) Lysosomal residence of cerium oxide nanoparticles in different cell lines upregulates the nanoparticles' oxidase activity, (d) leading to enhanced cytotoxicity. Panels (c) and (d) adapted with permission from Ref. 227. Copyright 2010 American Chemical Society.



and siRNA.<sup>223,224</sup> In order to improve the efficacy of photothermal ablation particularly for deep tissue therapy, gold nanorods were utilized along with an implantable source for the treatment of ovarian cancer in an orthotopic model.<sup>225</sup>

Endogenous activators of cytotoxic activity are often preferred, such as an i.v.-administered trigger or the tumor's innate features, since they allow clinicians to conduct therapy without deviating from well-established protocols and procedures. Toward this direction, Rotello and colleagues used chemical recognition to activate the cytotoxicity of cationic gold nanoparticles within cells.<sup>226</sup> Specifically, the positive charge of diamino-hexane-functionalized gold nanoparticles was neutralized via the capping of the nanoparticles with cucurbit[7]uril, allowing the nanoparticles to be endocytosed by the cells without any toxicity. Once the cells were treated with 1-adamantylamine, the nanoparticles dissociated from cucurbit[7]uril, and caused cell death, due to pore-forming capabilities of the nanoparticles' cationic groups [Fig. 5(b)]. Another research group used the intrinsic enzymatic properties of cerium oxide nanoparticles, where at physiological pH these nanoparticles behaved as antioxidant enzymes and at acidic microenvironments they acquired oxidase-like characteristics.<sup>227,228</sup> It was demonstrated that at physiological pH the nanoparticles scavenged reactive oxygen species, due to the conversion of cerium(III) to cerium(IV) and back to cerium(III). However at acidic pH, the nanoparticles did not undergo auto-regeneration, yet they catalyzed the oxidation of various substrates that ultimately led to cell death depending on the subcellular localization of these nanoparticles [Figs. 5(c) and 5(d)].<sup>229,230</sup>

## B. Emerging Nanotechnologies in Drug Delivery and Therapy

The continuous quest to identify new platforms for cancer therapy led to the introduction of new nanomaterials and innovative solutions, which ultimately may reach the patient's bedside. Carbon nanotubes, graphene, and fullerenes have been investigated due to their facile synthesis, unique

mechanical properties and multiple conjugation sites.<sup>231,232</sup> Surprisingly, many of these nanoparticles undergo renal clearance,<sup>133</sup> yet the initial circulation, solubility, and toxicity issues have been addressed with creative strategies, including PEGylation and nanoparticle surface modification. For instance, doxorubicin was effectively delivered to tumors with modified hydrophilic fullerenes that caused enhanced antitumor activity.<sup>233</sup> Recently, PEGylated graphene oxide nanoparticles delivered doxorubicin *in vitro*, where the drug was released by the late endosomes/lysosomes low pH, glutathione, and near-infrared light.<sup>234</sup> Carbon nanotubes were used for the delivery of topoisomerase inhibitors, such as camptothecin, irinotecan, and etoposide, and commonly used chemotherapeutics, like doxorubicin, paclitaxel, and tamoxifen.<sup>235</sup> Depending on the surface properties and chemical modifications of the carbon nanotubes, the drugs were retained through physical absorption or covalent bonds, which allowed drug release through pH changes, salt concentration differences, and esterases. Furthermore, since carbon nanotubes have a high aspect ratio and a large area with multiple conjugation sites, targeting moieties, including folic acid, cyclical RGD peptide, and antibodies, were introduced, allowing selective cytotoxicity toward certain cancer cell populations. In an innovative approach, Scheinberg and colleagues used single-wall carbon nanotubes for targeted radiotherapy, by conjugating to the nanoparticles an antibody and DOTA for the chelation of the alpha particle emitter <sup>225</sup>Ac.<sup>236</sup> Enhanced tumor regression was observed due to potency of the alpha particles, whereas the rapid clearance of the nanoparticles from circulation prevented systemic toxicity. Adopting similar conjugation strategies, single-wall carbon nanotubes delivered a peptide antigen to antigen-presenting cells *in vivo*, increasing the production of antibodies against the tumor-associated WT1 antigen that is found in many leukemias and cancers (Fig. 6).<sup>237</sup>

Apart from using nanoparticles as adjuvants and vaccinelike agents, engineered plant viruses are attractive drug delivery vehicles, since their production is affordable and scalable.<sup>238</sup> Among them, the cowpea mosaic virus was extensively studied, primarily due to high viral particle yield after plant infection

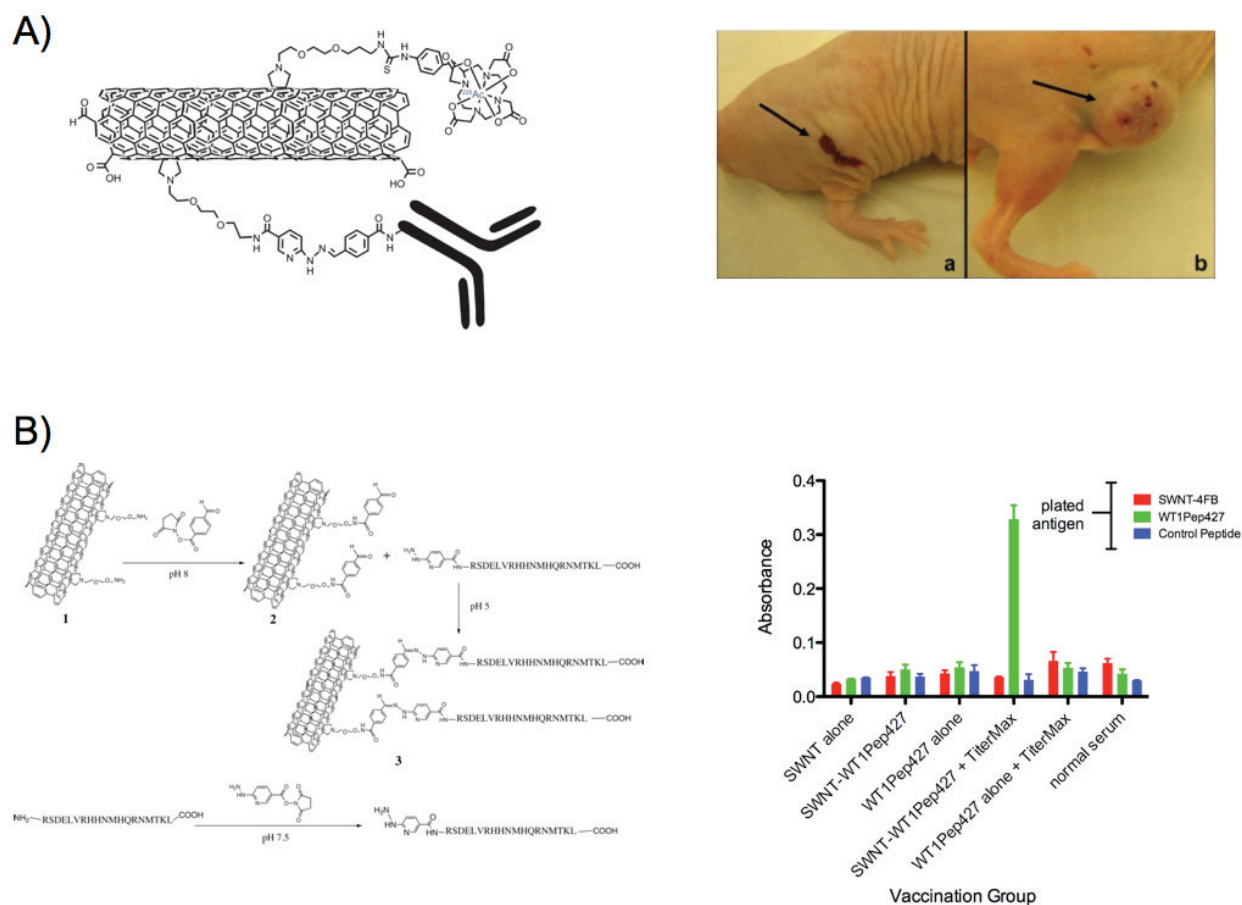


**FIG. 6:** Delivery of a peptide antigen with single-wall carbon nanotubes led to specific immune response toward the antigen *in vivo*, indicated by the levels of serum IgG that were quantified with ELISA. Adapted with permission from Ref. 237. Copyright 2011 American Chemical Society.

(1–2 g/kg), the viral capsid's thermal stability, and easy chemical modification of its coat proteins. This allowed the conjugation of small VEGFR1-targeting peptides and larger macromolecules, including enzymes, providing nanoparticles with different valency levels.<sup>239,240</sup> In model studies, up to 11 molecules of horseradish peroxidase (44 kDa) were conjugated on the surface of the cowpea mosaic virus, while low valency was achieved when glucose oxidase (160 kDa) was covalently attached via simple bioconjugation procedures. Several groups were able to deliver chemotherapeutics, like doxorubicin and proflavine, with the cargo either immobilized on the viral coat or retained within it

through hydrogen bonds between the viral RNA and guest molecule.<sup>241,242</sup> Steinmetz and colleagues were able to deliver infused chemotherapeutic cargo to a panel of cervical, breast, and colon cells with cowpea mosaic virions that utilized vimentin and underwent lysosomal degradation and drug release.<sup>242</sup> Other groups used the propensity of some alphaviruses toward tumors, and delivered diverse payload that ranged from small molecules and nucleic acids to proteins and gold nanoparticles.<sup>243</sup> The cargo was retained within the viral capsid, and was successfully released once within cancer cells, leaving healthy cells unaffected. However ongoing *in vivo* studies intend to address the immunogenic-

ity of plant viruses and improve the tumor uptake of these natural nanoparticles. Recent reports showed that the size and structure of the viruses play a key role in the nanoparticles' biodistribution and clearance.<sup>238,244</sup> Comparing the icosahedral cowpea mosaic virus (28 nm) and the filamentous potato virus X (515 × 13 nm), it was found that the elongated potato virus X demonstrated better tumor uptake and it was cleared by the spleen, contrary to the hepatic clearance of the cowpea mosaic virus. With the introduction of imaging agents,<sup>245,246</sup> the fate of these nanoparticles will be further delineated, assisting in their preclinical evaluation as multifunctional therapeutic vehicles.

With the introduction of new instrumentation and advancements in cancer biology, nanoparticles can support therapy and improve treatment outcome. Iron oxide nanoparticles were used as sensors for the detection of a single cancer cell in whole blood samples, by detecting aberrant expression of surface biomarkers [Fig. 7(a)].<sup>247</sup> Intriguingly, this unprecedented sensitivity was achieved with a multivalent small-molecule-conjugated magnetic nanosensor, which was able to quickly interrogate clinically relevant samples and potentially provide critical information on disease status, such as micrometastasis initiated by rare circulating tumor cells. Quantification of circulating tumor cells was also accomplished with micro-Hall detector and magnetic nanoparticles, using a creative microfluidic platform and a portable reader.<sup>248</sup> The nanosensors were able to determine the expression of prototypic biomarkers, such as EpCAM, HER2, and EGFR, on each detected cell, allowing the physician to characterize these metastasis progenitors and proceed to personalized therapy with administration of drugs that can target the corresponding oncogenic pathways. Further studies allowed the molecular profiling of cancer cells collected from fine-needle aspirates, using a biomarker-screening magnetic nanosensors panel [Fig. 7(b)].<sup>249</sup> Detection was accomplished with a portable micro-NMR sensor, which can be used in the clinic and at the patient bedside to quickly monitor molecular cascades related to disease progression and therapeutic interventions. Since sensitive probes are critical

in the translational success of new diagnostics and therapeutics, binding magnetic nanosensors were utilized to quantify the affinity and avidity of molecular entities toward receptors associated with disease pathogenesis [Fig. 7(c)].<sup>250</sup> This novel platform demonstrated that previously unidentified molecular interactions could be investigated with a solution-based optics-independent assay, thanks to the optimized display of the interrogated molecules and absence of steric hindrance. In an effort to model chemotherapeutic dynamics *ex vivo*, iron oxide nanoparticles were used to measure the binding of poly(ADP-ribose) polymerase (PARP) inhibitors to their target protein, which is differentially expressed in cancer cells.<sup>251</sup> Finally, since radiation therapy is widely used for the treatment of numerous cancers, cerium oxide nanoparticles were used for the selective cytoprotection of healthy cells, allowing ionizing radiation to affect only the malignant tissue.<sup>252–254</sup> To avoid potential nanoparticle side effects due to cerium's context-dependent self-regeneration and enzymatic activity, cerium oxide nanoparticles were introduced within an implantable device, which monitored the levels of reactive oxygen species generated by the inflammatory cascade and radiotherapy [Fig. 7(d)].<sup>255</sup> Detection was achieved through MRI and near-infrared fluorescence, since the high levels of reactive oxygen species caused clustered the device's iron oxide nanoparticles and quenched their fluorophore, opening new vistas in the management and treatment of cancer.

### III. CONCLUDING REMARKS

Nanoparticles provide exciting and promising new paradigms in diagnostic oncology and cancer therapeutics. For their successful transition to the clinic, it is important to thoroughly understand the interactions of these novel materials and architectures within the body, using suitable models and experimental strategies. With the advancements in nanomaterial design and tumor targeting, the use of innovative approaches to eradicate cancer cells, and the construction of multifunctional platforms that perform imaging and diagnosis, nanotechnology is

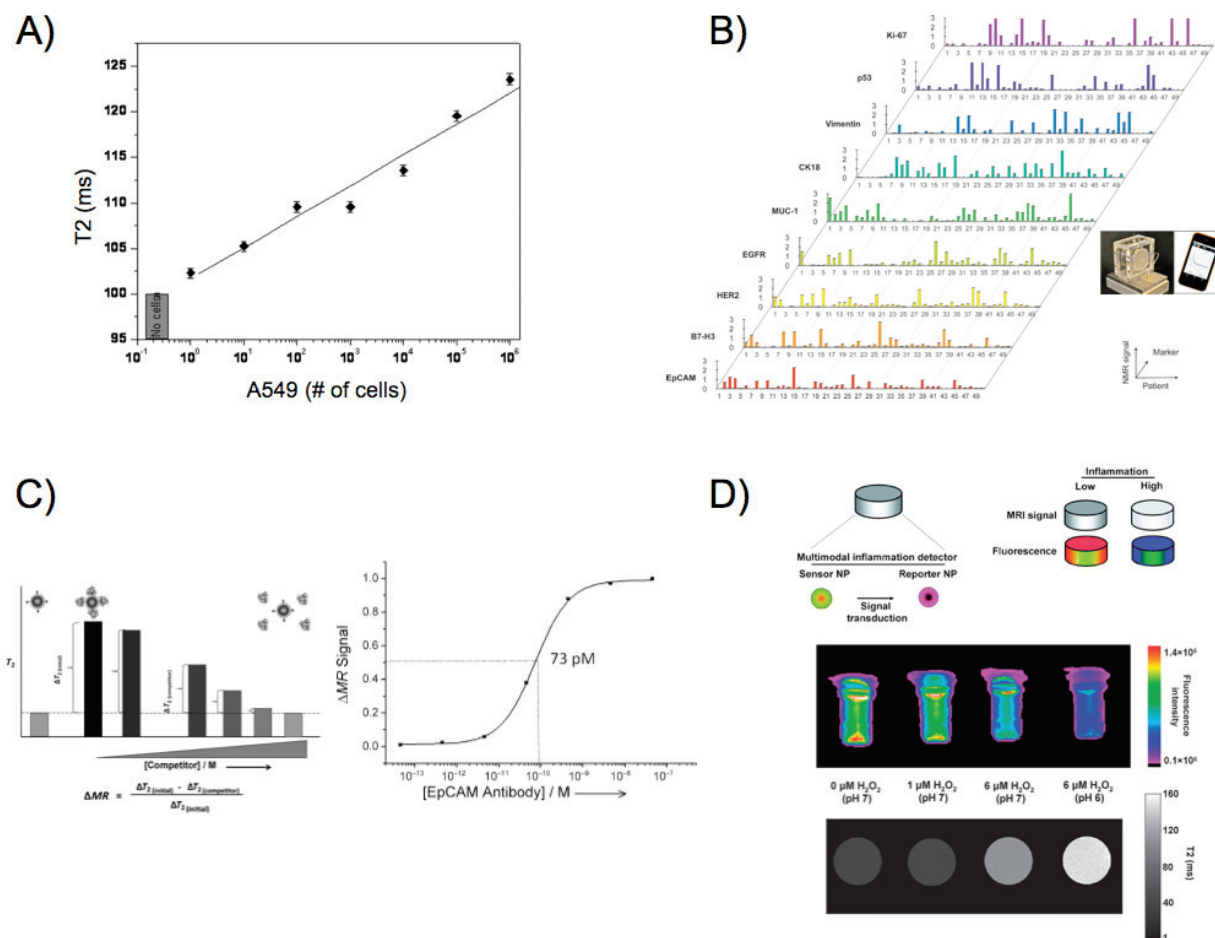


**FIG. 7:** (a) Small-molecule-displaying magnetic nanosensors quickly detected up to a single cancer cell in unprocessed blood samples, through changes in the sample's magnetic resonance signal. Adapted with permission from Ref. 247. Copyright 2009 American Chemical Society. (b) Detection of cancer biomarkers in clinical fine-needle aspirate samples using a micro-NMR instrument. Adapted with permission from Ref. 249. Copyright 2011 American Association for the Advancement of Science. (c) Binding magnetic nanodetectors determined the affinity between the cancer biomarker EpCAM and an anti-EpCAM antibody in suspension, as a model platform for investigating dynamic *in vivo* molecular interactions. Adapted with permission from Ref. 250. Copyright 2012 Wiley-VCH Verlag GmbH&Co. (d) A nanoparticle-based device monitored the levels of the archetype pro-inflammatory mediator H<sub>2</sub>O<sub>2</sub> through changes in the nanoparticles fluorescence and magnetic signal, using sensory and reporting nanoparticles. Adapted with permission from Ref. 255. Copyright 2012 Royal Society of Chemistry.

poised to improve cancer therapy, lower cancer mortality, and potentially lower the costs of treatment. In conjunction with new discoveries in cancer biology, nanoparticles delivering therapeutics and providing sensitive imaging will maximize tumor regression, minimize side effects, eliminate residual disease, and prevent metastasis, opening new frontiers in patient-tailored molecular oncology.

## ACKNOWLEDGMENTS

The authors acknowledge funding support from the Prostate Cancer Foundation and Alex Lemonade Foundation to C. Kaittanis. T.M. Shaffer is funded by a National Science Foundation Integrative Graduate Education and Research Traineeship (MAD, IGERT 0965983). D.Thorek and this work were supported by U.S. National

Institutes of Health (NIH) through the R25T Molecular Imaging Fellowship: Molecular Imaging Training in Oncology (5R25CA096945-07; Principal investigator H. Hricack). J. Grimm was supported in part by the Department of Defense Prostate Cancer Research Program of the Congressionally Directed Medical Research Programs under Award No. W81XWH-12-1-0509 (opinions, interpretations, conclusions, and recommendations are those of the author and are not necessarily endorsed by the funding agency), the Starr Cancer Consortium (Grant No. I4-A427), NIH (Grants No. P30 CA008748-44 S5 and No. 1R01EB014944), and the Louis V. Gerstner Young Investigator Award. Technical services provided by the Animal Imaging Core Facility were supported in part by grants from the NIH (Grants No. R24 CA083084 and No. P30 CA008748).

## REFERENCES

- Grimm J, Scheinberg DA. Will nanotechnology influence targeted cancer therapy? *Semin Radiat Oncol.* 2011;21:80-7.
- Tassa C, Duffner JL, Lewis TA, Weissleder R, Schreiber SL, Koehler AN, Shaw SY. Binding affinity and kinetic analysis of targeted small molecule-modified nanoparticles. *Bioconjug Chem.* 2010;21:14-9.
- Lichtman JW, Conchello JA. Fluorescence microscopy. *Nat Methods.* 2005;2:910-9.
- Kairdolf BA, Smith AM, Stokes TH, Wang MD, Young AN, Nie S. Semiconductor quantum dots for bioimaging and biodiagnostic applications. *Annu Rev Anal Chem (Palo Alto Calif).* 2013;6:143-62.
- Michalet X, Pinaud FF, Bentolila LA, Tsay JM, Doose S, Li JJ, Sundaresan G, Wu AM, Gambhir SS, Weiss S. Quantum dots for live cells, *in vivo* imaging, and diagnostics. *Science.* 2005;307:538-44.
- Resch-Genger U, Grabolle M, Cavaliere-Jaricot S, Nitschke R, Nann T. Quantum dots versus organic dyes as fluorescent labels. *Nat Methods.* 2008;5:763-75.
- Tokumasu F, Dvorak J. Development and application of quantum dots for immunocytochemistry of human erythrocytes. *J Microsc.* 2003;211:256-61.
- Li W, Nava RG, Bribriescio AC, Zinselmeyer BH, Spahn JH, Gelman AE, Krupnick AS, Miller MJ, Kreisel D. Intravital 2-photon imaging of leukocyte trafficking in beating heart. *J Clin Invest.* 2012;122:2499-508.
- Larson DR, Zipfel WR, Williams RM, Clark SW, Bruchez MP, Wise FW, Webb WW. Water-soluble quantum dots for multiphoton fluorescence imaging *in vivo*. *Science.* 2003;300:1434-6.
- Derfus AM, Chan WCW, Bhatia SN. Probing the cytotoxicity of semiconductor quantum dots. *Nano Lett.* 2004;4:11-8.
- Hardman R. A toxicologic review of quantum dots: toxicity depends on physicochemical and environmental factors. *Environ Health Persp.* 2006;114:165-72.
- Kosaka N, Ogawa M, Sato N, Choyke PL, Kobayashi H. *In vivo* real-time, multicolor, quantum dot lymphatic imaging. *J Invest Dermatol.* 2009;129:2818-22.
- Thorek DL, Ogirala A, Beattie BJ, Grimm J. Quantitative imaging of disease signatures through radioactive decay signal conversion. *Nat Med.* 2013;19:1345-50.
- Cai WB, Shin DW, Chen K, Gheysens O, Cao QZ, Wang SX, Gambhir SS, Chen XY. Peptide-labeled near-infrared quantum dots for imaging tumor vasculature in living subjects. *Nano Lett.* 2006;6:669-76.
- Gao XH, Cui YY, Levenson RM, Chung LWK, Nie SM. *In vivo* cancer targeting and imaging with semiconductor quantum dots. *Nat Biotechnol.* 2004;22:969-76.
- Liu W, Howarth M, Greytak AB, Zheng Y, Nocera DG, Ting AY, Bawendi MG. Compact biocompatible quantum dots functionalized for cellular imaging. *J Am Chem Soc.* 2008;130:1274-84.
- Breus VV, Heyes CD, Tron K, Nienhaus GU. Zwitterionic biocompatible quantum dots for

- wide pH stability and weak nonspecific binding to cells. *ACS Nano*. 2009;3:2573–80.
18. Ow H, Larson DR, Srivastava M, Baird BA, Webb WW, Wiesner U. Bright and stable core-shell fluorescent silica nanoparticles. *Nano Lett*. 2005;5:113–7.
  19. Ma K, Werner-Zwanziger U, Zwanziger J, Wiesner U. Controlling growth of ultrasmall sub- 10 nm fluorescent mesoporous silica nanoparticles. *Chem Mater*. 2013;25:677–91.
  20. Burns A, Ow H, Wiesner U. Fluorescent core-shell silica nanoparticles: towards “Lab on a Particle” architectures for nanobiotechnology. *Chem Soc Rev*. 2006;35:1028–42.
  21. Benezra M, Penate-Medina O, Zanzonico PB, Schaer D, Ow H, Burns A, DeStanchina E, Longo V, Herz E, Iyer S, Wolchok J, Larson SM, Wiesner U, Bradbury MS. Multimodal silica nanoparticles are effective cancer-targeted probes in a model of human melanoma. *J Clin Invest*. 2011;121:2768–80.
  22. Josephson L, Kircher MF, Mahmood U, Tang Y, Weissleder R. Near-infrared fluorescent nanoparticles as combined MR/optical imaging probes. *Bioconjug Chem*. 2002;13:554–60.
  23. van Schooneveld MM, Cormode DP, Koole R, van Wijngaarden JT, Calcagno C, Skajaa T, Hilhorst J, ‘t Hart DC, Fayad ZA, Mulder WJM, Meijerink A. A fluorescent, paramagnetic and PEGylated gold/silica nanoparticle for MRI, CT and fluorescence imaging. *Contrast Media Mol I*. 2010;5:231–6.
  24. Smith AM, Mancini MC, Nie SM. Bioimaging second window for *in vivo* imaging. *Nat Nanotechnol*. 2009;4:710–1.
  25. Weissleder R. A clearer vision for *in vivo* imaging. *Nat Biotechnol*. 2001;19:316–7.
  26. Kosuge H, Sherlock SP, Kitagawa T, Dash R, Robinson JT, Dai H, McConnell MV. Near infrared imaging and photothermal ablation of vascular inflammation using single-walled carbon nanotubes. *J Am Heart Assoc*. 2012;1:e002568.
  27. Welsher K, Liu Z, Sherlock SP, Robinson JT, Chen Z, Daranciang D, Dai H. A route to brightly fluorescent carbon nanotubes for near-infrared imaging in mice. *Nat Nanotechnol*. 2009;4:773–80.
  28. Orte A, Alvarez-Pez JM, Ruedas-Rama MJ. Fluorescence lifetime imaging microscopy for the detection of intracellular pH with quantum dot nanosensors. *ACS Nano*. 2013;7:6387–95.
  29. Wu T-J, Tzeng Y-K, Chang W-W, Cheng C-A, Kuo Y, Chien C-H, Chang H-C, Yu J. Tracking the engraftment and regenerative capabilities of transplanted lung stem cells using fluorescent nanodiamonds. *Nat Nanotechnol*. 2013;8:682–9.
  30. Campion A, Kambhampati P. Surface-enhanced Raman scattering. *Chem Soc Rev*. 1998;27:241–50.
  31. Nie S, Emory SR. Probing single molecules and single nanoparticles by surface-enhanced Raman scattering. *science*. 1997;275:1102–6.
  32. Qian J, Li X, Wei M, Gao XW, Xu ZP, He SL. Bio-molecule-conjugated fluorescent organically modified silica nanoparticles as optical probes for cancer cell imaging. *Opt Express*. 2008;16:19568–78.
  33. Wang Y, Yan B, Chen L. SERS tags: novel optical nanoprobe for bioanalysis. *Chem Rev*. 2012;113:1391–428.
  34. Zavaleta CL, Garai E, Liu JT, Sensarn S, Mandella MJ, Van de Sompel D, Friedland S, Van Dam J, Contag CH, Gambhir SS. A Raman-based endoscopic strategy for multiplexed molecular imaging. *Proc Natl Acad Sci U S A*. 2013;110:E2288–97.
  35. Kircher MF, de la Zerda A, Jokerst JV, Zavaleta CL, Kempen PJ, Mittra E, Pitter K, Huang R, Campos C, Habte F. A brain tumor molecular imaging strategy using a new triple-modality MRI-photoacoustic-Raman nanoparticle. *Nat Med*. 2012;18:829–34.
  36. Wang LV. Prospects of photoacoustic tomography. *Med Phys*. 2008;35:5758–67.
  37. Wang LV, Hu S. Photoacoustic tomography: *in vivo* imaging from organelles to organs. *Science*. 2012;335:1458–62.

38. Shashkov EV, Everts M, Galanzha EI, Zharov VP. Quantum dots as multimodal photoacoustic and photothermal contrast agents. *Nano Lett.* 2008;8:3953–8.
39. De La Zerda A, Zavaleta C, Keren S, Vaithilingam S, Bodapati S, Liu Z, Levi J, Smith BR, Ma TJ, Oralkan O, Cheng Z, Chen XY, Dai HJ, Khuri-Yakub BT, Gambhir SS. Carbon nanotubes as photoacoustic molecular imaging agents in living mice. *Nat Nanotechnol.* 2008;3:557–62.
40. Kim C, Cho EC, Chen J, Song KH, Au L, Favazza C, Zhang Q, Cogley CM, Gao F, Xia Y, Wang LV. *In vivo* molecular photoacoustic tomography of melanomas targeted by bioconjugated gold nanocages. *ACS Nano.* 2010;4:4559–64.
41. Zhang Q, Iwakuma N, Sharma P, Moudgil BM, Wu C, McNeill J, Jiang H, Grobmyer SR. Gold nanoparticles as a contrast agent for *in vivo* tumor imaging with photoacoustic tomography. *Nanotechnology.* 2009;20:395102.
42. Garcia-Allende PB, Glatz J, Koch M, Ntziachristos V. Enriching the interventional vision of cancer with fluorescence and optoacoustic imaging. *Journal of Nuclear Medicine.* 2013;54:664–7.
43. Wiener E, Brechbiel M, Brothers H, Magin R, Gansow O, Tomalia D, Lauterbur P. Dendrimer-based metal chelates: A new class of magnetic resonance imaging contrast agents. *Magn Reson Med.* 1994;31:1–8.
44. Svenson S, Tomalia DA. Dendrimers in biomedical applications-reflections on the field. *Adv Drug Deliv Rev.* 2012;57:2106–29.
45. Langereis S, de Lussanet QG, van Genderen MH, Meijer E, Beets-Tan RG, Griffioen AW, van Engelshoven J, Backes WH. Evaluation of Gd (III) DTPA-terminated poly (propylene imine) dendrimers as contrast agents for MR imaging. *NMR Biomed.* 2006;19:133–41.
46. Swanson SD, Kukowska-Latallo JF, Patri AK, Chen C, Ge S, Cao Z, Kotlyar A, East AT, Baker JR. Targeted gadolinium-loaded dendrimer nanoparticles for tumor-specific magnetic resonance contrast enhancement. *Int J Nanomed.* 2008;3:]:201–10.
47. Konda SD, Aref M, Wang S, Brechbiel M, Wiener EC. Specific targeting of folate-dendrimer MRI contrast agents to the high affinity folate receptor expressed in ovarian tumor xenografts. *magnetic resonance materials in physics, Biol Med.* 2001;12:104–13.
48. Han L, Li J, Huang S, Huang R, Liu S, Hu X, Yi P, Shan D, Wang X, Lei H. Peptide-conjugated polyamidoamine dendrimer as a nanoscale tumor-targeted T1 magnetic resonance imaging contrast agent. *Biomaterials.* 2011;32:2989–98.
49. Cheng Z, Thorek DL, Tsourkas A. Gadolinium-conjugated dendrimer nanoclusters as a tumor-targeted T1 magnetic resonance imaging contrast agent. *Angew Chem Int Ed.* 2010;49:346–50.
50. Margerum LD, Campion BK, Koo M, Shargill N, Lai J-J, Marumoto A, Christian Sontum P. Gadolinium (III) DO3A macrocycles and polyethylene glycol coupled to dendrimers: effect of molecular weight on physical and biological properties of macromolecular magnetic resonance imaging contrast agents. *J Alloys Compounds.* 1997;249:185–90.
51. Kabalka G, Buonocore E, Hubner K, Moss T, Norley N, Huang L. Gadolinium-labeled liposomes: targeted MR contrast agents for the liver and spleen. *Radiology.* 1987;163:255–8.
52. Ghaghada KB, Ravoori M, Sabapathy D, Bankson J, Kundra V, Annapragada A. New dual mode gadolinium nanoparticle contrast agent for magnetic resonance imaging. *PLoS One.* 2009;4:e7628.
53. Cheng Z, Thorek DL, Tsourkas A. Porous polymersomes with encapsulated Gd-labeled dendrimers as highly efficient MRI contrast agents. *Adv Funct Mater.* 2009;19:3753–9.
54. Cheng Z, Elias DR, Kamat NP, Johnston ED, Poloukhine A, Popik V, Hammer DA, Tsourkas A. Improved tumor targeting of polymer-based

- nanovesicles using polymer-lipid blends. *Bioconjug Chem.* 2011;22:2021–9.
55. Cheng Z, Tsourkas A. Paramagnetic porous polymersomes. *Langmuir.* 2008;24:8169–73.
  56. Gilad AA, Walczak P, McMahon MT, Na HB, Lee JH, An K, Hyeon T, van Zijl P, Bulte JW. MR tracking of transplanted cells with “positive contrast” using manganese oxide nanoparticles. *Magn Reson Med.* 2008;60:1–7.
  57. Shin J, Anisur RM, Ko MK, Im GH, Lee JH, Lee IS. Hollow manganese oxide nanoparticles as multifunctional agents for magnetic resonance imaging and drug delivery. *Angew Chem Int Ed.* 2009;48:321–4.
  58. Shapiro EM, Koretsky AP. Convertible manganese contrast for molecular and cellular MRI. *Magn Reson Med.* 2008;60:265–9.
  59. Weissleder R, Stark D, Engelstad B, Bacon B, Compton C, White D, Jacobs P, Lewis J. Superparamagnetic iron oxide: pharmacokinetics and toxicity. *Am J Roentgenol.* 1989;152:167–73.
  60. Arbab AS, Yocum GT, Kalish H, Jordan EK, Anderson SA, Khakoo AY, Read EJ, Frank JA. Efficient magnetic cell labeling with protamine sulfate complexed to ferumoxides for cellular MRI. *Blood.* 2004;104:1217–23.
  61. Thorek D, Elias DR, Tsourkas A. Comparative analysis of nanoparticle-antibody conjugations: carbodiimide versus click chemistry. *Mol Imaging.* 2008;8:221–9.
  62. Huber DL. Synthesis, properties, and applications of iron nanoparticles. *Small.* 2005;1:482–501.
  63. Bulte JW, Douglas T, Witwer B, Zhang S-C, Strable E, Lewis BK, Zywicke H, Miller B, van Gelderen P, Moskowitz BM. Magnetodendrimers allow endosomal magnetic labeling and *in vivo* tracking of stem cells. *Nat Biotechnol.* 2001;19:1141–7.
  64. Chen M, Yamamuro S, Farrell D, Majetich SA. Gold-coated iron nanoparticles for biomedical applications. *J Appl Phys.* 2003;93:7551–3.
  65. Lu Y, Yin Y, Mayers BT, Xia Y. Modifying the surface properties of superparamagnetic iron oxide nanoparticles through a sol-gel approach. *Nano Lett.* 2002;2:183–6.
  66. Stark D, Weissleder R, Elizondo G, Hahn P, Saini S, Todd L, Wittenberg J, Ferrucci J. Superparamagnetic iron oxide: clinical application as a contrast agent for MR imaging of the liver. *Radiology.* 1988;168:297–301.
  67. Weissleder R, Hahn P, Stark D, Elizondo G, Saini S, Todd L, Wittenberg J, Ferrucci J. Superparamagnetic iron oxide: enhanced detection of focal splenic tumors with MR imaging. *Radiology.* 1988;169:399–403.
  68. de Vries IJM, Lesterhuis WJ, Barentsz JO, Verdijk P, van Krieken JH, Boerman OC, Oyen WJ, Bonenkamp JJ, Boezeman JB, Adema GJ. Magnetic resonance tracking of dendritic cells in melanoma patients for monitoring of cellular therapy. *Nat Biotechnol.* 2005;23:1407–13.
  69. Thorek DL, Tsao PY, Arora V, Zhou L, Eisenberg RA, Tsourkas A. *In vivo*, multimodal imaging of B cell distribution and response to antibody immunotherapy in mice. *PLoS One.* 2010;5:e10655.
  70. Zhu J, Zhou L, XingWu F. Tracking neural stem cells in patients with brain trauma. *New Engl J Med.* 2006;355:2376–8.
  71. Magnitsky S, Watson D, Walton R, Pickup S, Bulte J, Wolfe J, Poptani H. *In vivo* and *ex vivo* MRI detection of localized and disseminated neural stem cell grafts in the mouse brain. *Neuroimage.* 2005;26:744–54.
  72. Heyn C, Bowen CV, Rutt BK, Foster PJ. Detection threshold of single SPIO-labeled cells with FIESTA. *Magn Reson Med.* 2005;53:312–20.
  73. Kircher MF, Gambhir SS, Grimm J. Noninvasive cell-tracking methods. *Nat Rev Clin Oncol.* 2011;8:677–88.
  74. Weissleder R, Kelly K, Sun EY, Shtatland T, Josephson L. Cell-specific targeting of nanoparticles by multivalent attachment of small molecules. *Nat Biotechnol.* 2005;23:1418–23.
  75. Thorek DL, Tsourkas A. Size, charge and concentration dependent uptake of iron oxide



- particles by non-phagocytic cells. *Biomaterials*. 2008;29:3583–90.
76. Ogden SG, Lewis D, Shapter JG. Silane functionalisation of iron oxide nanoparticles. *Smart materials, nano- and micro-smart systems*. Bellingham, WA: SPIE; 2008. p. 72670A-A-11.
77. Tavitian B, Trébossen R, Pasqualini R, Dollé F. *In vivo* radiotracer imaging. *Textbook of in vivo imaging in vertebrates*. Hoboken: Wiley; 2007. p. 103–47.
78. Som P, Atkins HL, Bandoypadhyay D, Fowler JS, MacGregor RR, Matsui K, Oster ZH, Sacker DF, Shiue CY, Turner H, Wan CN, Wolf AP, Zabinski SV. A fluorinated glucose analog, 2-fluoro-2-deoxy-D-glucose (F-18): nontoxic tracer for rapid tumor detection. *Journal of Nuclear Medicine*. 1980;21:670–5.
79. Zanzonico P. Principles of nuclear medicine imaging: planar, SPECT, PET, multi-modality, and autoradiography systems. *Radiat Res*. 2012;177:349–64.
80. Alberti C. From molecular imaging in preclinical/clinical oncology to theranostic applications in targeted tumor therapy. *Eur Rev Med Pharmacol Sci*. 2012;16:1925–33.
81. Greish K. Enhanced permeability and retention of macromolecular drugs in solid tumors: a royal gate for targeted anticancer nanomedicines. *J Drug Targeting*. 2007;15:457–64.
82. Albanese A, Tang PS, Chan WCW. The effect of nanoparticle size, shape, and surface chemistry on biological systems. *Annu Rev Biomed Eng*. 2012;14:1–16.
83. Werner ME, Karve S, Sukumar R, Cummings ND, Copp JA, Chen RC, Zhang T, Wang AZ. Folate-targeted nanoparticle delivery of chemo- and radiotherapeutics for the treatment of ovarian cancer peritoneal metastasis. *Biomaterials*. 2011;32:8548–54.
84. Pressly ED, Pierce RA, Connal LA, Hawker CJ, Liu Y. Nanoparticle PET/CT imaging of natriuretic peptide clearance receptor in prostate cancer. *Bioconjug Chem*. 2013;24:196–204.
85. Sa LT, Pessoa C, Meira AS, da Silva MI, Missailidis S, Santos-Oliveira R. Development of nanoaptamers using a mesoporous silica model labeled with (99m)Tc for cancer targeting. *Oncology*. 2012;82:213–7.
86. Zhang MZ, Yu RN, Chen J, Ma ZY, Zhao YD. Targeted quantum dots fluorescence probes functionalized with aptamer and peptide for transferrin receptor on tumor cells. *Nanotechnology*. 2012;23:485104.
87. Karmani L, Labar D, Valembois V, Bouchat V, Nagaswaran PG, Bol A, Gillart J, Leveque P, Bouzin C, Bonifazi D, Michiels C, Feron O, Gregoire V, Lucas S, Borghet TV, Gallez B. Antibody-functionalized nanoparticles for imaging cancer: influence of conjugation to gold nanoparticles on the biodistribution of <sup>89</sup>Zr-labeled cetuximab in mice. *Contrast Media Mol I*. 2013;8:402–8.
88. Abou DS, Thorek DL, Ramos NN, Pinkse MW, Wolterbeek HT, Carlin SD, Beattie BJ, Lewis JS. (89)Zr-labeled paramagnetic octreotide-liposomes for PET-MR imaging of cancer. *Pharm Res*. 2013;30:878–88.
89. Hermanson GT. *Bioconjugate techniques*. 2 ed. New York: Academic Press; 2010.
90. Kalia J, Raines RT. Advances in bioconjugation. *Curr Organic Chem*. 2010;14:138–47.
91. Kaisin G, Corentin W, Andre L. Fluorine-18 labeling of biocompatible nanoparticles for PET imaging. *J Label Compounds Radiopharm*. 2013;56:S250.
92. Bailey DL, Willowson KP. An evidence-based review of quantitative SPECT imaging and potential clinical applications. *J Nucl Med*. 2013;54:83–9.
93. Sharma R, Xu Y, Kim SW, Schueller MJ, Alexoff D, Smith SD, Wang W, Schlyer D. Carbon-11 radiolabeling of iron-oxide nanoparticles for dual-modality PET/MR imaging. *Nanoscale*. 2013;5:7476–83.
94. Yang M, Cheng K, Qi S, Liu H, Jiang Y, Jiang H, Li J, Chen K, Zhang H, Cheng Z. Affibody modified and radiolabeled gold-Iron

- oxide hetero-nanostructures for tumor PET, optical and MR imaging. *Biomaterials*. 2013;34:2796–806.
95. Hong H, Chen F, Cai W. Pharmacokinetic issues of imaging with nanoparticles: focusing on carbon nanotubes and quantum dots. *Mol Imaging Biol*. 2013;15:507–20.
  96. McDevitt MR, Chattopadhyay D, Jaggi JS, Finn RD, Zanzonico PB, Villa C, Rey D, Mendenhall J, Batt CA, Njardarson JT, Scheinberg DA. PET imaging of soluble yttrium-86-labeled carbon nanotubes in mice. *PLoS One*. 2007;2:e907.
  97. Wong AW, Ormsby E, Zhang H, Seo JW, Mahakian LM, Caskey CF, Ferrara KW. A comparison of image contrast with (64)Cu-labeled long circulating liposomes and (18)F-FDG in a murine model of mammary carcinoma. *Am J Nucl Med Mol Imaging*. 2013;3:32–43.
  98. Duconge F, Pons T, Pestourie C, Herin L, Theze B, Gombert K, Mahler B, Hinnen F, Kuhnast B, Dolle F, Dubertret B, Tavitian B. Fluorine-18-labeled phospholipid quantum dot micelles for *in vivo* multimodal imaging from whole body to cellular scales. *Bioconjug Chem*. 2008;19:1921–6.
  99. Schipper ML, Cheng Z, Lee SW, Bentolila LA, Iyer G, Rao J, Chen X, Wu AM, Weiss S, Gambhir SS. microPET-based biodistribution of quantum dots in living mice. *J Nucl Med*. 2007;48:1511–8.
  100. Guo J, Hong H, Chen G, Shi S, Zheng Q, Zhang Y, Theuer CP, Barnhart TE, Cai W, Gong S. Image-guided and tumor-targeted drug delivery with radiolabeled unimolecular micelles *Biomaterials*. 2013;34:8323–32.
  101. James ML, Gambhir SS. A molecular imaging primer: modalities, imaging agents, and applications. *Physiol Rev*. 2012;92:897–965.
  102. Yamamoto Y, Nishiyama Y, Satoh K, Ohkawa M, Kameyama K, Hayashi E, Tanabe M. Comparative evaluation of Tc-99m MIBI and Tl-201 chloride SPECT in non-small-cell lung cancer mediastinal lymph node metastases. *Clin Nucl Med*. 2000;25:29–32.
  103. Sandiford L, Phinikaridou A, Protti A, Meszaros LK, Cui X, Yan Y, Frodsham G, Williamson PA, Gaddum N, Botnar RM, Blower PJ, Green MA, de Rosales RTM. Bisphosphonate-anchored PEGylation and radiolabeling of superparamagnetic iron oxide: long-circulating nanoparticles for *in vivo* multimodal (T1 MRI-SPECT) imaging. *ACS Nano*. 2013;7:500–12.
  104. Barrefelt AA, Brismar TB, Egri G, Aspelin P, Olsson A, Oddo L, Margheritelli S, Caidahl K, Paradossi G, Dahne L, Axelsson R, Hassan M. Multimodality imaging using SPECT/CT and MRI and ligand functionalized 99mTc-labeled magnetic microbubbles. *EJNMMI Res*. 2013;3:12.
  105. Li S, Goins B, Zhang L, Bao A. Novel multifunctional theranostic liposome drug delivery system: construction, characterization, and multimodality MR, near-infrared fluorescent, and nuclear imaging. *Bioconjug Chem*. 2012;23:1322–32.
  106. Huang F-YJ, Lee T-W, Kao C-HK, Chang C-H, Zhang X, Lee W-Y, Chen W-J, Wang S-C, Lo J-M. Imaging, Autoradiography, and biodistribution of Re-188-labeled PEGylated nanoliposome in orthotopic glioma bearing rat model. *Cancer Biother Radiopharm*. 2011;26:717–25.
  107. Cheng CC, Huang CF, Ho AS, Peng CL, Chang CC, Mai FD, Chen LY, Luo TY, Chang J. Novel targeted nuclear imaging agent for gastric cancer diagnosis: glucose-regulated protein 78 binding peptide-guided 111In-labeled polymeric micelles. *Int J Nanomed*. 2013;8:1385–91.
  108. Peng CL, Shih YH, Lee PC, Hsieh TM, Luo TY, Shieh MJ. Multimodal image-guided photothermal therapy mediated by 188Re-labeled micelles containing a cyanine-type photosensitizer. *ACS Nano*. 2011;5:5594–607.
  109. Zeng D, Zeglis BM, Lewis JS, Anderson CJ. The growing impact of bioorthogonal click chemistry on the development of radiopharmaceuticals. *J Nucl Med*. 2013;54:829–32.

110. Zeglis BM, Sevak KK, Reiner T, Mohindra P, Carlin SD, Zanzonico P, Weissleder R, Lewis JS. A pretargeted PET imaging strategy based on bioorthogonal Diels-Alder click chemistry. *J Nucl Med.* 2013;54:1389–96.
111. Mulvey JJ, Villa CH, McDevitt MR, Escorcía FE, Casey E, Scheinberg DA. Self-assembly of carbon nanotubes and antibodies on tumours for targeted amplified delivery. *Nat Nanotechnol.* 2013;8:763–71.
112. Zavaleta CL, Hartman KB, Miao Z, James ML, Kempen P, Thakor AS, Nielsen CH, Sinclair R, Cheng Z, Gambhir SS. Preclinical evaluation of Raman nanoparticle biodistribution for their potential use in clinical endoscopy imaging. *Small.* 2011;7:2232–40.
113. Mohs AM, Mancini MC, Singhal S, Provenzale JM, Leyland-Jones B, Wang MD, Nie S. Hand-held spectroscopic device for *in vivo* and intraoperative tumor detection: contrast enhancement, detection sensitivity, and tissue penetration. *Anal Chem.* 2010;82:9058–65.
114. Wang Y, Liu Y, Luehmann H, Xia X, Wan D, Cutler C, Xia Y. Radioluminescent gold nanocages with controlled radioactivity for real-time *in vivo* imaging. *Nano Lett.* 2013;13:581–5.
115. American Cancer Society. *Cancer Facts Figures 2013.*
116. Hanahan D, Weinberg RA. Hallmarks of cancer: the next generation. *Cell.* 2011;144:646–74.
117. Ferrari M. Cancer nanotechnology: opportunities and challenges. *Nat Rev Cancer.* 2005;5:161–71.
118. Scheinberg DA, Villa CH, Escorcía FE, McDevitt MR. Conscripts of the infinite armada: systemic cancer therapy using nanomaterials. *Nat Rev Clin Oncol.* 2010;7:266–76.
119. Schroeder A, Heller DA, Winslow MM, Dahlman JE, Pratt GW, Langer R, Jacks T, Anderson DG. Treating metastatic cancer with nanotechnology. *Nat Rev Cancer.* 2012;12:39–50.
120. Marty JJ, Oppenheim RC, Speiser P. Nanoparticles—new colloidal drug delivery system. *Pharm Acta Helv.* 1978;53:17–23.
121. Verma RK, Garg S. Current status of drug delivery technologies and future directions. *Pharm Technol On-line.* 2001;25:1–14.
122. Almeida AJ, Souto E. Solid lipid nanoparticles as a drug delivery system for peptides and proteins. *Adv Drug Deliv Rev.* 2007;59:478–90.
123. Hartman KB, Wilson LJ, Rosenblum MG. Detecting and treating cancer with nanotechnology. *Mol Diagn Ther.* 2008;12:1–14.
124. Davis ME, Chen Z, Shin DM. Nanoparticle therapeutics: an emerging treatment modality for cancer. *Nat Rev Drug Discov.* 2008;7:771–82.
125. Ferrari M. Beyond drug delivery. *Nat Nanotechnol.* 2008;3:131–2.
126. Chithrani BD, Ghazani AA, Chan WCW. Determining the size and shape dependence of gold nanoparticle uptake into mammalian cells. *Nano Lett.* 2006;6:662–8.
127. Jiang W, Kim BYS, Rutka JT, Chan WCW. Nanoparticle-mediated cellular response is size-dependent. *Nat Nanotechnol.* 2008;3:145–50.
128. Gratton SEA, Ropp PA, Pohlhaus PD, Luft JC, Madden VJ, Napier ME, DeSimone JM. The effect of particle design on cellular internalization pathways. *Proc Natl Acad Sci U S A.* 2008;105:11613–8.
129. Fifiş T, Gamvrellis A, Crimeen-Irwin B, Pietersz GA, Li J, Mottram PL, McKenzie IFC, Plebanski M. Size-dependent immunogenicity: Therapeutic and protective properties of nano-vaccines against tumors. *J Immunol.* 2004;173:3148–54.
130. Tran KK, Shen H. The role of phagosomal pH on the size-dependent efficiency of cross-presentation by dendritic cells. *Biomaterials.* 2009;30:1356–62.
131. Decuzzi P, Ferrari M. The receptor-mediated endocytosis of nonspherical particles. *Biophys J.* 2008;94:3790–7.

132. Jin H, Heller DA, Sharma R, Strano MS. Size-dependent cellular uptake and expulsion of single-walled carbon nanotubes: single particle tracking and a generic uptake model for nanoparticles. *ACS Nano*. 2009;3:149–58.
133. Ruggiero A, Villa CH, Bander E, Rey DA, Bergkvist M, Batt CA, Manova-Todorova K, Deen WM, Scheinberg DA, McDevitt MR. Paradoxical glomerular filtration of carbon nanotubes. *Proc Natl Acad Sci U S A*. 2010;107:12369–74.
134. Gref R, Minamitake Y, Peracchia MT, Trubetskoy V, Torchilin V, Langer R. Biodegradable long-circulating polymeric nanospheres. *Science*. 1994;263:1600–3.
135. Torchilin VP, Trubetskoy VS, Milshteyn AM, Canillo J, Wolf GL, Papisov MI, Bogdanov AA, Narula J, Khaw BA, Omelyanenko VG. Targeted Delivery of diagnostic agents by surface-modified liposomes. *J Control Release*. 1994;28:45–58.
136. Yamashita F, Hashida M. Pharmacokinetic considerations for targeted drug delivery. *Adv Drug Deliv Rev*. 2013;65:139–47.
137. Adisheshaiah PP, Hall JB, McNeil SE. Nanomaterial standards for efficacy and toxicity assessment. *Wires Nanomed Nanobi*. 2010;2:99–112.
138. Gottesman MM, Fojo T, Bates SE. Multidrug resistance in cancer: role of ATP-dependent transporters. *Nat Rev Cancer*. 2002;2:48–58.
139. Park JW, Hong KL, Kirpotin DB, Colbern G, Shalaby R, Baselga J, Shao Y, Nielsen UB, Marks JD, Moore D, Papahadjopoulos D, Benz CC. Anti-HER2 immunoliposomes: enhanced efficacy attributable to targeted delivery. *Clin Cancer Res*. 2002;8:1172–81.
140. Couvreur P, Kante B, Roland M, Speiser P. Adsorption of anti-neoplastic drugs to polyalkylcyanoacrylate nanoparticles and their release in calf serum. *J Pharm Sci*. 1979;68:1521–4.
141. Duncan R. Polymer conjugates as anti-cancer nanomedicines. *Nat Rev Cancer*. 2006;6:688–701.
142. Duncan R, Vicent MJ. Polymer therapeutics—prospects for 21st century: the end of the beginning. *Adv Drug Deliv Rev*. 2013;65:60–70.
143. Kopeček J, Bazilova H. Poly[N-(2-hydroxypropyl)methacrylamide]. 1. radical polymerization and copolymerization. *Eur Polym J*. 1973;9:7–14.
144. Vasey PA, Kaye SB, Morrison R, Twelves C, Wilson P, Duncan R, Thomson AH, Murray LS, Hilditch TE, Murray T, Burtles S, Fraier D, Frigerio E, Cassidy J, Comm CRCPII. Phase I clinical and pharmacokinetic study of PK1 [N-(2-hydroxypropyl)methacrylamide copolymer doxorubicin]: first member of a new class of chemotherapeutic agents—drug-polymer conjugates. *Clin Cancer Res*. 1999;5:83–94.
145. Mitra A, Coleman T, Borgman M, Nan A, Ghandehari H, Line BR. Polymeric conjugates of mono- and bi-cyclic alpha(V)beta(3) binding peptides for tumor targeting. *J Control Release*. 2006;114:175–83.
146. Mitra A, Mulholland J, Nan A, McNeill E, Ghandehari H, Line BR. Targeting tumor angiogenic vasculature using polymer-RGD conjugates. *J Control Release*. 2005;102:191–201.
147. Zhang Y, Chan HF, Leong KW. Advanced materials and processing for drug delivery: The past and the future. *Adv Drug Deliv Rev*. 2013;65:104–20.
148. Yoo HS, Lee KH, Oh JE, Park TG. *In vitro* and *in vivo* anti-tumor activities of nanoparticles based on doxorubicin-PLGA conjugates. *J Control Release*. 2000;68:419–31.
149. Panyam J, Dali MA, Sahoo SK, Ma WX, Chakravarthi SS, Amidon GL, Levy RJ, Labhasetwar V. Polymer degradation and *in vitro* release of a model protein from poly(D,L-lactide-co-glycolide) nano- and microparticles. *J Control Release*. 2003;92:173–87.
150. Panyam J, Zhou WZ, Prabha S, Sahoo SK, Labhasetwar V. Rapid endo-lysosomal escape of poly(DL-lactide-co-glycolide) nanoparticles:

- implications for drug and gene delivery. *FASEB J*. 2002;n:16:1217-26.
151. Kranz H, Ubrich N, Maincent P, Bodmeier R. Physicomechanical properties of biodegradable poly(D,L-lactide) and poly(D,L-lactide-co-glycolide) films in the dry and wet states. *J Pharm Sci*. 2000;89:1558-66.
152. Tsuji H. Poly(lactide) stereocomplexes: Formation, structure, properties, degradation, and applications. *Macromol Biosci*. 2005;5:569-97.
153. Sengupta S, Eavarone D, Capila I, Zhao GL, Watson N, Kiziltepe T, Sasisekharan R. Temporal targeting of tumour cells and neovasculature with a nanoscale delivery system. *Nature*. 2005;436:568-72.
154. McCarthy JR, Perez JM, Bruckner C, Weissleder R. Polymeric nanoparticle preparation that eradicates tumors. *Nano Lett*. 2005;5:2552-6.
155. Hrkach J, Von Hoff D, Ali MM, Andrianova E, Auer J, Campbell T, De Witt D, Figa M, Figueiredo M, Horhota A, Low S, McDonnell K, Peeke E, Retnarajan B, Sabnis A, Schnipper E, Song JJ, Song YH, Summa J, Tompsett D, Troiano G, Hoven TV, Wright J, LoRusso P, Kantoff PW, Bander NH, Sweeney C, Farokhzad OC, Langer R, Zale S. Preclinical development and clinical translation of a PSMA-targeted docetaxel nanoparticle with a differentiated pharmacological profile. *Sci Transl Med*. 2012;4; 128ra39.
156. Lawson HC, Sampath P, Bohan E, Park MC, Hussain N, Olivi A, Weingart J, Kleinberg L, Brem H. Interstitial chemotherapy for malignant gliomas: the Johns Hopkins experience. *J Neuro-Oncol*. 2007;83:61-70.
157. Yokoyama M, Miyauchi M, Yamada N, Okano T, Sakurai Y, Kataoka K, Inoue S. Characterization and anticancer activity of the micelle-forming polymeric anticancer drug adriamycin-conjugated poly(ethylene glycol)-poly(aspartic acid) block copolymer. *Cancer Res*. 1990;50:1693-700.
158. Kabanov AV, Batrakova EV, Alakhov VY. Pluronic (R) block copolymers as novel poly-mer therapeutics for drug and gene delivery. *J Control Release*. 2002;82:189-212.
159. Santra S, Kaittanis C, Perez JM. Aliphatic hyperbranched polyester: a new building block in the construction of multifunctional nanoparticles and nanocomposites. *Langmuir*. 2010;26:5364-73.
160. Boohaker RJ, Zhang G, Lee MW, Nemecek KN, Santra S, Perez JM, Khaled AR. Rational development of a cytotoxic peptide to trigger cell death. *Mol Pharm*. 2012;9:2080-93.
161. Sun TM, Du JZ, Yao YD, Mao CQ, Dou S, Huang SY, Zhang PZ, Leong KW, Song EW, Wang J. Simultaneous delivery of siRNA and paclitaxel via a "two-in-one" micelleplex promotes synergistic tumor suppression. *ACS Nano*. 2011;5:1483-94.
162. Santra S, Kaittanis C, Perez JM. Cytochrome C encapsulating theranostic nanoparticles: a novel bifunctional system for targeted delivery of therapeutic membrane-impermeable proteins to tumors and imaging of cancer therapy. *Mol Pharm*. 2010;7:1209-22.
163. Garcia-Fuentes M, Alonso MJ. Chitosan-based drug nanocarriers: Where do we stand? *J Control Release*. 2012;161:496-504.
164. Paraskar AS, Soni S, Chin KT, Chaudhuri P, Muto KW, Berkowitz J, Handlogten MW, Alves NJ, Bilgicer B, Dinulescu DM, Mashelkar RA, Sengupta S. Harnessing structure-activity relationship to engineer a cisplatin nanoparticle for enhanced antitumor efficacy. *Proc Natl Acad Sci U S A*. 2010;107:12435-40.
165. Roh YH, Lee JB, Kiatwuthinon P, Hartman MR, Cha JJ, Um SH, Muller DA, Luo D. DNAsomes: multifunctional DNA-based nanocarriers. *Small*. 2011;7:74-8.
166. Li J, Pei H, Zhu B, Liang L, Wei M, He Y, Chen N, Li D, Huang Q, Fan CH. Self-assembled multivalent DNA nanostructures for noninvasive intracellular delivery of immunostimulatory CpG oligonucleotides. *ACS Nano*. 2011;5:8783-9.

167. Afonin KA, Grabow WW, Walker FM, Bindewald E, Dobrovolskaia MA, Shapiro BA, Jaeger L. Design and self-assembly of siRNA-functionalized RNA nanoparticles for use in automated nanomedicine. *Nat Protoc.* 2011;6:2022–34.
168. Andersen ES, Dong M, Nielsen MM, Jahn K, Subramani R, Mamdouh W, Golas MM, Sander B, Stark H, Oliveira CLP, Pedersen JS, Birkedal V, Besenbacher F, Gothelf KV, Kjems J. Self-assembly of a nanoscale DNA box with a controllable lid. *Nature.* 2009;459:73–6.
169. Ko SH, Liu HP, Chen Y, Mao CD. DNA nanotubes as combinatorial vehicles for cellular delivery. *Biomacromolecules.* 2008;9:3039–43.
170. Wilner OI, Orbach R, Henning A, Teller C, Yehezkeili O, Mertig M, Harries D, Willner I. Self-assembly of DNA nanotubes with controllable diameters. *Nat Commun.* 2011;2:540.
171. Douglas SM, Bachelet I, Church GM. A logic-gated nanorobot for targeted transport of molecular payloads. *Science.* 2012;335:831–4.
172. Frandsen JL, Ghandehari H. Recombinant protein-based polymers for advanced drug delivery. *Chem Soc Rev.* 2012;41:2696–706.
173. Megeed Z, Cappello J, Ghandehari H. Genetically engineered silk-elastinlike protein polymers for controlled drug delivery. *Adv Drug Deliv Rev.* 2002;54:1075–91.
174. Bangham AD, Standish MM, Watkins JC. Diffusion of univalent ions across the lamellae of swollen phospholipids. *J Mol Biol.* 1965;13:238–52.
175. Gregoriadis G, Ryman BE. Liposomes as carriers of enzymes or drugs: a new approach to the treatment of storage diseases. *Biochem J.* 1971;124:58p.
176. Torchilin VP. Recent advances with liposomes as pharmaceutical carriers. *Nat Rev Drug Discov.* 2005;4:145–60.
177. Cabanes A, Briggs KE, Gokhale PC, Treat JA, Rahman A. Comparative *in vivo* studies with paclitaxel and liposome-encapsulated paclitaxel. *Int J Oncol.* 1998;12:1035–40.
178. Allison RR, Downie GH, Cuenca R, Hu X-H, Childs CJ, Sibata CH. Photosensitizers in clinical PDT. *Photodiagn Photodyn Therapy.* 2004;1:27–42.
179. Tang W, Xu H, Kopelman R, Philbert MA. Photodynamic characterization and *in vitro* application of methylene blue-containing nanoparticle platforms. *Photochem Photobiol.* 2005;81:242–9.
180. Lovell JF, Jin CS, Huynh E, Jin H, Kim C, Rubinstein JL, Chan WC, Cao W, Wang LV, Zheng G. Porphysome nanovesicles generated by porphyrin bilayers for use as multimodal biophotonic contrast agents. *Nat Mater.* 2011;10:324–32.
181. Banerjee D, Sengupta S. Nanoparticles in cancer chemotherapy. *Prog Mol Biol Transl Sci.* 2011;104:489–507.
182. McIntosh TJ. The effect of cholesterol on the structure of phosphatidylcholine bilayers. *Biochim Biophys Acta.* 1978;513:43–58.
183. Cullis PR, Hope MJ. The bilayer stabilizing role of sphingomyelin in the presence of cholesterol: a 31P NMR study. *Biochim Biophys Acta.* 1980;597:533–42.
184. Allen TM, Cullis PR. Liposomal drug delivery systems: from concept to clinical applications. *Adv Drug Deliv Rev.* 2013;65:36–48.
185. Ishida T, Iden DL, Allen TM. A combinatorial approach to producing sterically stabilized (Stealth) immunoliposomal drugs. *FEBS Lett.* 1999;460:129–33.
186. Iden DL, Allen TM. *In vitro* and *in vivo* comparison of immunoliposomes made by conventional coupling techniques with those made by a new post-insertion approach. *Biochim Biophys Acta.* 2001;1513:207–16.
187. Kluza E, van der Schaft DWJ, Hautvast PAI, Mulder WJM, Mayo KH, Griffioen AW, Strijkers GJ, Nicolay K. Synergistic targeting of  $\alpha(v)\beta(3)$  integrin and galectin-1 with heteromultivalent paramagnetic liposomes

- for combined MR imaging and treatment of angiogenesis. *Nano Lett.* 2010;10:52–8.
188. Nasongkla N, Shuai X, Ai H, Weinberg BD, Pink J, Boothman DA, Gao JM. cRGD-functionalized polymer micelles for targeted doxorubicin delivery. *Angew Chem Int Edit.* 2004;43:6323–7.
189. Suzuki R, Takizawa T, Kuwata Y, Mutoh M, Ishiguro N, Utoguchi N, Shinohara A, Eriguchi M, Yanagie H, Maruyama K. Effective anti-tumor activity of oxaliplatin encapsulated in transferrin-PEG-liposome. *Int J Pharm.* 2008;346:143–50.
190. Nellis DF, Giardina SL, Janini GM, Shenoy SR, Marks JD, Tsai R, Drummond DC, Hong K, Park JW, Ouellette TF, Perkins SC, Kirpotin DB. Preclinical manufacture of anti-HER2 liposome-inserting, scFv-PEG-Lipid conjugate. 2. conjugate micelle identity, purity, stability, and potency analysis. *Biotechnol Progr.* 2005;21:221–32.
191. Wicki A, Rochlitz C, Orleth A, Ritschard R, Albrecht I, Herrmann R, Christofori G, Mamot C. Targeting tumor-associated endothelial cells: anti-VEGFR2 immunoliposomes mediate tumor vessel disruption and inhibit tumor growth. *Clin Cancer Res.* 2012;18:454–64.
192. Mamot C, Drummond DC, Noble CO, Kallab V, Guo ZX, Hong KL, Kirpotin DB, Park JW. Epidermal growth factor receptor-targeted immunoliposomes significantly enhance the efficacy of multiple anticancer drugs *in vivo*. *Cancer Res.* 2005;65:11631–8.
193. Hussain S, Pluckthun A, Allen TM, Zangemeister-Wittke U. Antitumor activity of an epithelial cell adhesion molecule-targeted nanovesicular drug delivery system. *Mol Cancer Ther.* 2007;6:3019–27.
194. Straubinger RM, Papahadjopoulos D. Liposomes as carriers for intracellular delivery of nucleic acids. *Method Enzymol.* 1983;101:512–27.
195. Huang SL, MacDonald RC. Acoustically active liposomes for drug encapsulation and ultrasound-triggered release. *Biochim Biophys Acta.* 2004;1665:134–41.
196. Sarkar NR, Rosendahl T, Krueger AB, Banerjee AL, Benton K, Mallik S, Srivastava DK. “Uncorking” of liposomes by matrix metalloproteinase-9. *Chem Commun.* 2005:999–1001.
197. Weinstein JN, Magin RL, Yatvin MB, Zaharko DS. Liposomes and local hyperthermia—selective delivery of methotrexate to heated tumors. *Science.* 1979;204:188–91.
198. Yatvin MB, Kreutz W, Horwitz BA, Shinitzky M. Ph-Sensitive liposomes—possible clinical implications. *Science.* 1980;210:1253–4.
199. Kaittanis C, Santra S, Perez JM. Emerging nanotechnology-based strategies for the identification of microbial pathogenesis. *Adv Drug Deliv Rev.* 2010;62:408–23.
200. Maeng JH, Lee DH, Jung KH, Bae YH, Park IS, Jeong S, Jeon YS, Shim CK, Kim W, Kim J, Lee J, Lee YM, Kim JH, Kim WH, Hong SS. Multifunctional doxorubicin loaded superparamagnetic iron oxide nanoparticles for chemotherapy and magnetic resonance imaging in liver cancer. *Biomaterials.* 2010;31:4995–5006.
201. Dobson J. Magnetic nanoparticles for drug delivery. *Drug Dev Res.* 2006;67:55–60.
202. Alexiou C, Arnold W, Klein RJ, Parak FG, Hulin P, Bergemann C, Erhardt W, Wagenpfeil S, Luebke AS. Locoregional cancer treatment with magnetic drug targeting. *Cancer Res.* 2000;60:6641–8.
203. Hergt R, Dutz S, Müller R, Zeisberger M. Magnetic particle hyperthermia: nanoparticle magnetism and materials development for cancer therapy. *J Phy Condens Matter.* 2006;18:S2919.
204. Jordan A, Scholz R, Wust P, Fähling H, Krause J, Wlodarczyk W, Sander B, Vogl T, Felix R. Effects of magnetic fluid hyperthermia (MFH) on C3H mammary carcinoma *in vivo*. *Int J Hypertherm.* 1997;13:587–605.
205. Johannsen M, Thiesen B, Jordan A, Taymoorian K, Gneveckow U, Waldöfner N, Scholz R, Koch M, Lein M, Jung K. Magnetic fluid hyperthermia (MFH) reduces prostate cancer growth in the orthotopic Dunning R3327 rat model. *Prostate.* 2005;64:283–92.

206. Jordan A, Scholz R, Maier-Hauff K, van Landeghem FK, Waldoefner N, Teichgraber U, Pinkernelle J, Bruhn H, Neumann F, Thiesen B. The effect of thermotherapy using magnetic nanoparticles on rat malignant glioma. *J Neuro-Oncol.* 2006;78:7–14.
207. Maier-Hauff K, Rothe R, Scholz R, Gneveckow U, Wust P, Thiesen B, Feussner A, von Deimling A, Waldoefner N, Felix R. Intracranial thermotherapy using magnetic nanoparticles combined with external beam radiotherapy: results of a feasibility study on patients with glioblastoma multiforme. *J Neuro-Oncol.* 2007;81:53–60.
208. Thiesen B, Jordan A. Clinical applications of magnetic nanoparticles for hyperthermia. *Int J Hypertherm.* 2008;24:467–74.
209. Santra S, Kaittanis C, Grimm J, Perez JM. Drug/dye-loaded, multifunctional iron oxide nanoparticles for combined targeted cancer therapy and dual optical/magnetic resonance imaging. *Small.* 2009;5:1862–8.
210. Cheng K, Peng S, Xu C, Sun S. Porous hollow Fe(3)O(4) nanoparticles for targeted delivery and controlled release of cisplatin. *J Am Chem Soc.* 2009;131:10637–44.
211. Zhang F, Braun GB, Pallaoro A, Zhang Y, Shi Y, Cui D, Moskovits M, Zhao D, Stucky GD. Mesoporous multifunctional upconversion luminescent and magnetic “nanorattle” materials for targeted chemotherapy. *Nano Lett.* 2012;12:61–7.
212. Nasongkla N, Bey E, Ren J, Ai H, Khemtong C, Guthi JS, Chin SF, Sherry AD, Boothman DA, Gao J. Multifunctional polymeric micelles as cancer-targeted, MRI-ultrasensitive drug delivery systems. *Nano Lett.* 2006;6:2427–30.
213. Zhang XQ, Xu X, Lam R, Giljohann D, Ho D, Mirkin CA. Strategy for increasing drug solubility and efficacy through covalent attachment to polyvalent DNA-nanoparticle conjugates. *ACS Nano.* 2011;5:6962–70.
214. Kim CK, Ghosh P, Pagliuca C, Zhu ZJ, Menichetti S, Rotello VM. Entrapment of hydrophobic drugs in nanoparticle monolayers with efficient release into cancer cells. *J Am Chem Soc.* 2009;131:1360–1.
215. Cheng Y, A CS, Meyers JD, Panagopoulos I, Fei B, Burda C. Highly efficient drug delivery with gold nanoparticle vectors for *in vivo* photodynamic therapy of cancer. *J Am Chem Soc.* 2008;130:10643–7.
216. Agasti SS, Chompoosor A, You CC, Ghosh P, Kim CK, Rotello VM. Photoregulated release of caged anticancer drugs from gold nanoparticles. *J Am Chem Soc.* 2009;131:5728–9.
217. de la Rica R, Aili D, Stevens MM. Enzyme-responsive nanoparticles for drug release and diagnostics. *Adv Drug Deliv Rev.* 2012;64:967–78.
218. Timko BP, Dvir T, Kohane DS. Remotely triggerable drug delivery systems. *Adv Mater.* 2010;22:4925–43.
219. Park JH, Gu L, von Maltzahn G, Ruoslahti E, Bhatia SN, Sailor MJ. Biodegradable luminescent porous silicon nanoparticles for *in vivo* applications. *Nat Mater.* 2009;8:331–6.
220. Park JH, von Maltzahn G, Ong LL, Centrone A, Hatton TA, Ruoslahti E, Bhatia SN, Sailor MJ. Cooperative nanoparticles for tumor detection and photothermally triggered drug delivery. *Adv Mater.* 2010;22:880–5.
221. Yavuz MS, Cheng Y, Chen J, Cogley CM, Zhang Q, Rycenga M, Xie J, Kim C, Song KH, Schwartz, AG, Wang LV, Xia Y. Gold nanocages covered by smart polymers for controlled release with near-infrared light. *Nat Mater.* 2009;8:935–9.
222. Lu W, Xiong C, Zhang G, Huang Q, Zhang R, Zhang JZ, Li C. Targeted photothermal ablation of murine melanomas with melanocyte-stimulating hormone analog-conjugated hollow gold nanospheres. *Clin Cancer Res.* 2009;15:876–86.
223. Sun X, Zhang G, Keynton RS, O’Toole MG, Patel D, Gobin AM. Enhanced drug delivery via hyperthermal membrane disruption using targeted gold nanoparticles with PEGylated protein-G as a cofactor. *Nanomedicine.* 2013;9:1214–22.



224. Lu W, Zhang G, Zhang R, Flores LG, 2nd, Huang Q, Gelovani JG, Li C. Tumor site-specific silencing of NF-kappaB p65 by targeted hollow gold nanosphere-mediated photothermal transfection. *Cancer Res.* 2010;70:3177–88.
225. Bagley AF, Hill S, Rogers GS, Bhatia SN. Plasmonic photothermal heating of intraperitoneal tumors through the use of an implanted near-infrared source. *ACS Nano.* 2013;7:8089–97.
226. Kim C, Agasti SS, Zhu Z, Isaacs L, Rotello VM. Recognition-mediated activation of therapeutic gold nanoparticles inside living cells. *Nat Chem.* 2010;2:962–6.
227. Asati A, Santra S, Kaittanis C, Nath S, Perez JM. Oxidase-like activity of polymer-coated cerium oxide nanoparticles. *Angew Chem Int Ed Engl.* 2009;48:2308–12.
228. Kuchma MH, Komanski CB, Colon J, Teblum A, Masunov AE, Alvarado B, Babu S, Seal S, Summy J, Baker CH. Phosphate ester hydrolysis of biologically relevant molecules by cerium oxide nanoparticles. *Nanomedicine.* 2010;6:738–44.
229. Asati A, Kaittanis C, Santra S, Perez JM. pH-tunable oxidase-like activity of cerium oxide nanoparticles achieving sensitive fluorogenic detection of cancer biomarkers at neutral pH. *Anal Chem.* 2011;83:2547–53.
230. Asati A, Santra S, Kaittanis C, Perez JM. Surface-charge-dependent cell localization and cytotoxicity of cerium oxide nanoparticles. *ACS Nano.* 2010;4:5321–31.
231. Georgakilas V, Kordatos K, Prato M, Guldi DM, Holzinger M, Hirsch A. Organic functionalization of carbon nanotubes. *J Am Chem Soc.* 2002;124:760–1.
232. Kam NW, Dai H. Carbon nanotubes as intracellular protein transporters: generality and biological functionality. *J Am Chem Soc.* 2005;127:6021–6.
233. Chaudhuri P, Paraskar A, Soni S, Mashelkar RA, Sengupta S. Fullerenol-cytotoxic conjugates for cancer chemotherapy. *ACS Nano.* 2009;3:2505–14.
234. Kim H, Lee D, Kim J, Kim TI, Kim WJ. Photothermally triggered cytosolic drug delivery via endosome disruption using a functionalized reduced graphene oxide. *ACS Nano.* 2013;7:6735–46.
235. Wong BS, Yoong SL, Jagusiak A, Panczyk T, Ho HK, Ang WH, Pastorin G. Carbon nanotubes for delivery of small molecule drugs. *Adv Drug Deliv Rev.* 2013;65:1964–2015.
236. Ruggiero A, Villa CH, Holland JP, Sprinkle SR, May C, Lewis JS, Scheinberg DA, McDevitt MR. Imaging and treating tumor vasculature with targeted radiolabeled carbon nanotubes. *Int J Nanomedicine.* 2010;5:783–802.
237. Villa CH, Dao T, Ahearn I, Fehrenbacher N, Casey E, Rey DA, Korontsvit T, Zakhaleva V, Batt CA, Philips MR, Scheinberg DA. Single-walled carbon nanotubes deliver peptide antigen into dendritic cells and enhance IgG responses to tumor-associated antigens. *ACS Nano.* 2011;5:5300–11.
238. Steinmetz NF. Viral nanoparticles in drug delivery and imaging. *Mol Pharm.* 2013;10:1–2.
239. Brunel FM, Lewis JD, Destito G, Steinmetz NF, Manchester M, Stuhlmann H, Dawson PE. Hydrazone ligation strategy to assemble multifunctional viral nanoparticles for cell imaging and tumor targeting. *Nano Lett.* 2010;10:1093–7.
240. Aljabali AA, Barclay JE, Steinmetz NF, Lomonosoff GP, Evans DJ. Controlled immobilisation of active enzymes on the cowpea mosaic virus capsid. *Nanoscale.* 2012;4:5640–5.
241. Aljabali AA, Shukla S, Lomonosoff GP, Steinmetz NF, Evans DJ. CPMV-DOX delivers. *Mol Pharm.* 2013;10:3–10.
242. Yildiz I, Lee KL, Chen K, Shukla S, Steinmetz NF. Infusion of imaging and therapeutic molecules into the plant virus-based carrier cowpea mosaic virus: Cargo-loading and delivery. *J Control Release.* 2013;172:568–578.
243. Cheng F, Tsvetkova IB, Khuong YL, Moore AW, Arnold RJ, Goicochea NL, Dragnea B, Mukhopadhyay S. The packaging of different

- cargo into enveloped viral nanoparticles. *Mol Pharm*. 2013;10:51–8.
244. Shukla S, Wen AM, Ayat NR, Commandeur U, Gopalkrishnan R, Broome AM, Lozada KW, Keri RA, Steinmetz NF. Biodistribution and clearance of a filamentous plant virus in healthy and tumor-bearing mice. *Nanomedicine*. 2013;2014;9:221–35.
245. Bruckman MA, Hern S, Jiang K, Flask CA, Yu X, Steinmetz NF. Tobacco mosaic virus rods and spheres as supramolecular high-relaxivity MRI contrast agents. *J Mater Chem B*. 2013;1:1482–90.
246. Leong HS, Steinmetz NF, Ablack A, Destito G, Zijlstra A, Stuhlmann H, Manchester M, Lewis JD. Intravital imaging of embryonic and tumor neovasculature using viral nanoparticles. *Nat Protoc*. 2010;5:1406–17.
247. Kaittanis C, Santra S, Perez JM. Role of nanoparticle valency in the nondestructive magnetic-relaxation-mediated detection and magnetic isolation of cells in complex media. *J Am Chem Soc*. 2009;131:12780–91.
248. Issadore D, Chung J, Shao H, Liang M, Ghazani AA, Castro CM, Weissleder R, Lee H. Ultrasensitive clinical enumeration of rare cells *ex vivo* using a micro-hall detector. *Sci Transl Med*. 2012;4:141ra92.
249. Haun JB, Castro CM, Wang R, Peterson VM, Marinelli BS, Lee H, Weissleder R. Micro-NMR for rapid molecular analysis of human tumor samples. *Sci Transl Med*. 2011;3:71ra16.
250. Santiesteban OJ, Kaittanis C, Perez JM. Assessment of molecular interactions through magnetic relaxation. *Angew Chem Int Ed Engl*. 2012;51:6728–32.
251. Ullal AV, Reiner T, Yang KS, Gorbатов R, Min C, Issadore D, Lee H, Weissleder R. Nanoparticle-mediated measurement of target-drug binding in cancer cells. *ACS Nano*. 2011;5:9216–24.
252. Colon J, Herrera L, Smith J, Patil S, Komanski C, Kupelian P, Seal S, Jenkins DW, Baker CH. Protection from radiation-induced pneumonitis using cerium oxide nanoparticles. *Nanomedicine*. 2009;5:225–31.
253. Colon J, Hsieh N, Ferguson A, Kupelian P, Seal S, Jenkins DW, Baker CH. Cerium oxide nanoparticles protect gastrointestinal epithelium from radiation-induced damage by reduction of reactive oxygen species and upregulation of superoxide dismutase 2. *Nanomedicine*. 2010;6:698–705.
254. Wason MS, Colon J, Das S, Seal S, Turkson J, Zhao J, Baker CH. Sensitization of pancreatic cancer cells to radiation by cerium oxide nanoparticle-induced ROS production. *Nanomedicine*. 2013;9:558–69.
255. Kaittanis C, Santra S, Asati A, Perez JM. A cerium oxide nanoparticle-based device for the detection of chronic inflammation via optical and magnetic resonance imaging. *Nanoscale*. 2012;4:2117–23.